FRACTIONAL ORDER CONTROL IN HAPTICS

by

OZAN TOKATLI

Submitted to the Graduate School of Engineering and Natural Sciences
in partial fulfillment of the requirements
for the degree of Doctor of Philosophy

in Sabancı University

August 2015

Fractional Order Control in Haptics

APPROVED BY:

Assoc. Prof. Dr. Volkan Patoğlu (Thesis Advisor)	.....
Assoc. Prof. Dr. Kemalettin Erbatur	.....
Assoc. Prof. Dr. Nihat Gökhan Göğüş	.....
Assist. Prof. Dr. Mehmet Can Dede	.....
Assist. Prof. Dr. Özkan Bebek	.....

DATE OF APPROVAL: 04.08.2015

ABSTRACT

FRACTIONAL ORDER CONTROL IN HAPTICS

by

Ozan Tokatlı

Supervisor: Volkan Patoğlu

Fractional order (FO) calculus—a generalization of the traditional calculus to arbitrary order differointegration—is an effective mathematical tool that broadens the modeling boundaries of the familiar integer order calculus. The effectiveness of this remarkable mathematical tool has been observed in many practical applications. For instance, FO models enable faithful representation of viscoelastic materials that exhibit frequency dependent stiffness and damping characteristics within a single mechanical element.

In this dissertation, we propose and analyze the use of FO controllers in haptic systems and provide a systematic analysis of this new control method in the light of the fundamental trade-off between the stability robustness and the transparency performance. FO controllers provide a promising generalization that allows one to better shape the frequency response of a system to achieve more favorable robustness and performance characteristics. In particular, the use of FO calculus in systems and control applications provides the user with an extra design variable, the order of differointegration, which can be tuned to improve the desired behavior of the overall system.

We introduce a generalized FO nondimensionalized sampled-data model for the haptic system and study its frequency dependent behaviour. Then, we analyze the stability of this system with and without a human operator in the loop. Moreover, we experimentally verify the stability analysis and demonstrate that the experiments

capture the essence of the stability behaviour between different differentiation orders.

The passivity analysis is conducted for two cases: the first approach takes the environment model into account and ensures the passivity of the haptic system together with the virtual environment, while the second approach assumes the presence of a passive environment model in the control loop and introduces a controller to the closed-loop system that acts like a buffer between the haptic display and the virtual environment. The second approach is more suitable for complex environments as it investigates the passivity properties of the two-port haptic system together with a virtual coupler.

After characterizing the stability boundaries for the FO haptic system, we analyse the performance of the system by studying the transparency performance of the haptic rendering with such controllers. In particular, we employ effective impedance analysis to decompose the closed-loop impedance of a haptic system into its parts and study the contribution of FO elements on the stiffness and damping rendering characteristics of the system.

Finally, we apply the theoretical results to a novel haptic rendering scenario: haptic rendering of viscoelastic materials. A fractional order mathematical model for the human prostate tissue with history depended stress and deflection behavior, is chosen as the viscoelastic physical system to be rendered. The stress relaxation of the haptic rendering is verified against the experimental data, indicating a high fidelity rendering.

ÖZETÇE

HAPTIKTE KESIR DERECELI DENETIM

Ozan Tokatlı

Danışman: Volkan Patoğlu

Geleneksel kalkülüsün bir genelleştirmesi olan kesir dereceli kalkülüs, matematiksel modelleminin sınırlarını genişleten önemli bir araçtır. Bu çarpıcı matematiksel aracın etkinliği birçok uygulamada gözlemlenmiştir. Örneğin, viskoelastik malzemelerin başarılı bir şekilde modellenmesi, özellikle de frakansa dayalı esneklik ve sönümlemenin tek bir mekanik eleman olarak temsil edilebilmesi, kesir dereceli kalkülüs ile mümkün olmuştur.

Bu doktora tezinde, kesir dereceli denetleyicilerin haptik sistemlerde kullanılmasını öneriyor ve bu denetleyicilerin kullanımıyla ilgili olarak gerekli analizleri, haptik sistemlerde görülen, kararlılık gürbüzlüğü-şeffaflık ödünleşimi açısından ele alıyoruz. Kesir dereceli denetleyiciler, var olan denetleyici modellerining genelleştirmesini sunarken, sistemin frekans cevabını daha iyi gürbüzlük ve başarım elde edecek şekilde değiştirme açısından da ümit verici sonuçlar vermektedir. Özellikle, kesir dereceli denetleyicilerin kullanımıyla birlikte, kullanıcı fazladan bir tasarım değişkenine (türevin derecesi) sahip olmaktadır ve bu değişkeni toplam sistemin davranışını ayarlamak kullanabilmektedir.

Bu doktora tezinde, genelleştirilmiş, kesir dereceli, boyutsuz ve örneklenmiş dizge modelini haptik sistemler için öneriyoruz ve bu yapının frekansa dayalı davranışını inceliyoruz. Bu incelemelerde öncelikle sistemin kararlılık analizi yapılmaktadır. Kararlılık analizinde haptik sistemi kullanan insanın olduğu ve olmadığı durumlar ele alınmıştır. Ayrıca, kararlılık analizi, farklı türev dereceleri için deneysel olarak da doğrulanmıştır ve deney sonuçları, kağıt üzerinde yapılan analizin genel yapısı ile niteliksel

olarak uyumludur.

Haptik sistemin pasiflik analizi iki durum için yapılmıştır. İlk durumda sanal çevre modeli de haptik sistemin pasiflik analizine dahil edilmiştir. Öte yandan, ikinci durumda ise pasif olduğu bilgisi dışında başka bir bilgi bulunmayan sanal çevreler için haptik sistemin pasiflik analizi yapılmıştır. İkinci durumda kullanılan denetleyici mimarisi, ilk durumunkine göre farklılıklar içermektedir. İkinci durumda, haptik robot ile sanal çevre bir birlerine sanal bağlayıcı yardımı ile bağlanmıştır. Sanal bağlayıcı, tampon bölge gibi davranmaktadır. İkinci yöntem, karmaşık sanal çevre modelleri ile çalışmak için daha uygun bir denetim mimarisidir, çünkü haptik sistem ve sanal bağlayıcının pasifliğinin sağlandığı durumlarda pasif insan ve sanal çevre için pasif bir toplam haptik sistem elde edilebilmektedir.

Kesir dereceli haptik sistemin kararlılık karakterizasyonundan yapıldıktan sonra haptik sistemin şeffaflık başarımı incelenmiştir. Bu analizde efektif empedans analizi yöntemi kullanılmıştır. Bu yöntem, kapalı döngü haptik sistemin empedans aktarım işlevini reel ve karmaşık parçalarına ayırmakta ve bu şekilde kesir dereceli denetleyicinin gerçeklenen esnemeye ve sönümlemeye olan katkıları incelemektedir.

Son olarak, teorik sonuçlarımızı, yeni bir haptik gerçekleme örneğinde kullandık. Bu haptik uygulamada viskoelastik malzeme özelliğine sahip olan insan prostatı gerçeklenmiştir. İnsan prostatı için kesir dereceli mateatiksel model bulunmaktadır. Bu model, prostatın sergilediği geçmişe dayalı hareketleri doğru olarak modelleyebilmektedir. Bu geçmişe dayalı hareketler stres rahatlaması ve sünme etkisidir. Gerçeklemede, haptik sistemde gözlenen stres rahatlaması, gerçek dokunun deneysel sonuçlarıyla karşılaştırılmıştır ve gerçeklemenin başarımı gözlenmiştir.

ACKNOWLEDGEMENTS

It is a great pleasure to extend my gratitude to my thesis advisor Assist. Prof. Dr. Volkan Patoğlu for his precious guidance and support. I am greatly indebted to him for his supervision and excellent advises throughout my PhD study. I would gratefully thank Assoc. Prof. Dr. Kemalettin Erbatur, Assist. Prof. Dr. Mehmet Can Dede and Assit. Prof. Dr. Özkan Bebek for their feedbacks and spending their valuable time to serve as my jurors.

I would like to acknowledge the financial support provided by The Scientific & Technological Research Council of Turkey (TÜBİTAK) through my PhD education under BİDEB scholarship.

Many thanks to my friends for making the laboratory enjoyable and memorable and I would also like to thank my family for all their love and support throughout my life.

Finally, a heartfelt thanks goes to my girlfriend Damla Arifoğlu. I could not imagine finishing this thesis if it were her constant love, support and faith in me through all those hard times. Without her everything, including this thesis, would be incomplete.

TABLE OF CONTENTS

LIST OF FIGURES . . . . . **ix**

CHAPTER

I. INTRODUCTION 1
1.1 Contribution of the Dissertation 3
II. RELATED WORK 6
2.1 Stability and Passivity of Haptic Displays 6
2.2 Transparency of Haptic Systems 9
2.3 Fractional Order Control 11
III. PRELIMINARIES 13
3.1 Haptic System 13
3.2 Fractional Order Control 15
3.3 Virtual Environment 19
3.4 Nondimensionalization of the System Parameters 20
3.5 Characterization of the Virtual Environment 20
3.6 Passivity of Haptic System 23
3.6.1 Haptic System in One Port Network Form 23
3.6.2 Haptic Systems in Two Port Network Form 24
IV. STABILITY ANALYSIS AND EXPERIMENTAL VERIFICATION 25
4.1 Discrete-Time Transfer Functions 25
4.2 Stability Analysis 26
4.3 Stability Regions 26
4.4 Testbed and Experiments 28
4.5 Comparison 30
4.6 Sensitivity of Stability Regions to Changes in Model Parameters 31
4.7 Case Study 33
4.8 Discussion 34
4.9 Conclusions 35
V. PASSIVITY OF THE HAPTIC SYSTEM 36
5.1 Haptic System in One Port Network Form 37
5.2 Haptic System in Two Port Network Form 39
5.3 Discussion 41
5.4 Conclusions 42

VI. TRANSPARENCY ANALYSIS 43
6.1 Conclusion 46
VII. HAPTIC RENDERING OF HUMAN PROSTATE 47
VIII. CONCLUSION AND FUTURE WORK 50

BIBLIOGRAPHY **52**

LIST OF FIGURES

3.1 The sampled-data haptic system with ideal sampler and zero order hold. 14
3.2 The model of the haptic interface 14
3.3 Coefficients that scale effective stiffness and damping of the fractional order virtual environment 21
3.4 Effective stiffness and damping of the fractional order virtual environment of Eq. 3.8. 22
3.5 One port network representation of a haptic system 23
3.6 Two port network representation of a haptic system with virtual coupling 24

4.1 Stability region of haptic system for various differentiation orders . . . 28
4.2 Single DoF voice coil actuated haptic display 29
4.3 Results of Z-width experiments of the haptic system 30
4.4 Stability regions for different differentiation orders, under changes in non-dimensional parameters δ and γ. 32
4.5 Sensitivity transfer function of the fractional order haptic system for different differentiation orders μ 34

5.1 Nondimensional passivity regions for different values of differentiation order μ 39

6.1 Change of the interval of ωT with respect to μ 44
6.2 Effective impedance of a haptic system with $m = 0.65$ kg, $b = 3.5$ N s/mm, $K = 50$ N/m, $B = 1$ N s/m for various differentiation orders . 46

7.1 Voice coil actuators used in the stress relaxation experiments 48
7.2 Stress relaxation of the cancerous prostate tissue 49

CHAPTER I

INTRODUCTION

The goal of haptic rendering is to synthetically create virtual environments as close to reality as possible, while simultaneously ensuring safety of the interaction between the human operator and the haptic display. However, there is a well-known trade-off between the stability robustness and the transparency of interaction and there exists a continual search for new approaches to improve the rendering quality of the haptic systems, while ensuring coupled stability of interaction.

While the environments to be rendered can vary widely, ranging from rigid bodies to elastic materials, and even to fluids, the stability robustness has been most commonly studied for the simplest environment model that consists of a linear spring and a damper. This model has been shown to capture many important aspects of haptic rendering, from the sampled-data nature of the haptic systems to the presence of the human operator in the loop.

The classical linear elastic models can be used to capture the natural behavior of many environments; however, these models fall short of capturing some other important natural phenomenon, such as time dependent stress relaxation of viscoelastic elements, a crucial aspect required to faithfully model mammal tissue. In particular, viscoelastic materials display elasticity and viscosity properties simultaneously, generalizing the existing theories for solids and viscous materials. Modeling the complex behavior of viscoelastic materials is an active research area and it has been recognized that fractional order calculus is an effective tool to model these materials with fewer parameters and

simpler mathematical structures [1]. For instance, the standard linear solid (SLS) model has been shown to faithfully model human prostate tissue [2], since this model is capable of capturing the time dependent creep compliance property of the tissue. Another application of fractional order modeling of mammal tissue can be found in [3] where a fractional order Kelvin-Voight model is used for the modeling of the liver tissue.

Inspired by the existence of fractional order models in the nature, we propose the use of fractional order models/controllers in haptic systems. We generalize the existing results based on linear elastic and viscous mechanical elements to models with linear fractional order elements. The fractional order model not only can recover the classical virtual environment model of consisting of springs and dampers, but also enable rendering of realistic viscoelastic materials thanks to the fractional order differointegration term in its model.

Fractional order calculus is a generalization of the familiar integer order calculus in that it allows for differentiation/integration, called differointegration, with orders of *any real number*. Intuitively, a fractional order derivative behaves as an interpolation between the neighboring integer order derivatives, due the continuous behavior of the differointegration operator with respect to its order. For instance, considering position signal as the input, continually varying the order of differentiation order from 1 to 0 acts as changing the properties of a linear mechanical element from a pure dissipation element towards a pure potential energy storage (stiffness) element. Likewise, tuning the differentiation order from 1 to 2 acts as continually transforming from a pure dissipation element towards a pure kinetic energy storage (inertia) element. Note that dissipation exits for all differentiation orders in the open interval $(0, 2)$, while pure energy storage takes place only for the integer orders of 0 and 2.

The use of fractional order calculus in systems and control applications is known to provide the user with an extra parameter, the order of differointegration, which can be tuned to improve the desired behaviour of the overall system. This property of fractional

order controllers is widely employed for robust motion control applications. For haptic systems, introducing a proper amount of dissipation is essential for achieving coupled stability, as well as improving their transient response during interactions. However, dissipation can adversely affect the transparency of the rendering by distorting the match between the desired and rendered impedance values. Fractional calculus based control is a promising generalization in that it provides an alternative means for tuning the characteristics of the dissipation supplied to the system, through the adjustment of the order of differentiation. In particular, since the fractional calculus generalization provides an additional degree of freedom for adjusting the dissipation behaviour of the overall system, fractional order haptic rendering has the potential to improve upon the stability robustness-transparency trade-off dictated by the integer order analysis.

Along these lines, we study haptic rendering of fractional order impedances and explore how the use of fractional order elements impacts various aspects of haptic systems such as uncoupled stability, passivity and closed-loop effective impedance. Our results generalize the well-known conditions of stability and passivity to include fractional order impedances and demonstrate the effect of the order of differointegration on stability. Rendering quality of such fractional order impedances is also analyzed in terms of effective impedances and the effects of using fractional order differeointegration is investigated. Even though there has been an investigation of haptic rendering of viscoelastic materials in [4], an extensive study of the stability, passivity, transparency of fractional order models and extensions to virtual couplers with these new controller have not been studied to the best of authors' knowledge.

1.1 Contribution of the Dissertation

This dissertation proposes the use of fractional order control in haptic systems and analyzes stability, passivity and transparency characteristics of fractional order controllers in a human-in-the-loop haptic system. We also provide a novel haptic rendering exam-

ple for viscoelastic materials. The contributions of this work are:

- We propose the use of fractional order control, which utilizes arbitrary order differointegrals in the control loop, in haptic systems.
- Based on a simple virtual environment model consisting of a linear spring and a fractional order dissipation element, we analyze the frequency dependent behavior of this new virtual environment in terms of its effective stiffness and damping characteristics.
- We generalize the existing nondimensionalization of the haptic system parameters and introduce an appropriate nondimensionalization for the fractional order dissipation element.
- We investigate the stability of the fractional order haptic system with and without the human in the loop. To study qualitative effects of having human in the loop, we utilize a second order linear model for the human and study effects of parameter changes on the stability regions.
- We experimentally verify the stability of the system in the absence of human operator and we demonstrate that the theoretical analysis is consistent with the experimental results.
- We analyze the passivity of the haptic system, in sampled-data system form, with the fractional order virtual environment model. We generalize the passivity condition in the literature developed for spring-damper type virtual environment to spring-fractional order damper type virtual environment model. We show that this generalization can successfully recover the existing condition.
- We also extended the passivity analysis of the haptic system to complex, but passive, environments. We show that the haptic system with a fractional order virtual coupler can be made passive for certain differentiation orders.

- We analyze the transparency performance of the closed-loop haptic system in terms of its effective stiffness and damping and show that stiffness rendering with a dissipative element of order less than 1 can help improve the stiffness rendering quality, while an order greater than 1 can introduce higher dissipation for high frequencies.

- Finally, we present a novel haptic rendering example, that extends virtual environment to viscoelastic materials. In particular, we demonstrate a successful haptic rendering of prostate tissue, which exhibits fractional order dynamics. The stress relaxation of the virtual prostate model is verified to overlap with the experimental results of real prostate tissue.

CHAPTER II

RELATED WORK

The aim of this dissertation is to introduce fractional order control to haptics. Therefore, before any mathematical analysis, a thorough literature survey is necessary to build a solid background. In the literature, the reader can find the related work on stability of haptic systems with explicit human model, passivity and other robust stability based techniques in haptics, transparency analysis of haptic systems and fractional order calculus and its applications to control problems.

2.1 Stability and Passivity of Haptic Displays

A haptic system is desired to stay stable at all times, for any human operator, and under any operation/grip conditions. The presence of the human operator in the loop significantly complicates the coupled stability analysis and controller design of haptic systems. The first and the foremost challenge is to find a simple and reliable model for the human operator. Without a model of the human operator, determining the coupled stability of the haptic system is not a trivial task. Furthermore, the sampled-data nature of the haptic systems introduces an extra challenge to the analysis.

The coupled stability analysis of haptic systems can be loosely categorized into two different approaches. The first, approach assumes a model for the human operator and checks for the overall stability of the system based on this model. On the other hand, the second approach, focuses on the haptic system alone and aims at robust stability of the haptic system for a certain, but wide, range of human operator models.

Analyzing the stability of haptic systems was one of the focuses of the early haptic research. Despite the lack of human operator model, researchers have assumed simple models, generally second order linear models, representing the human operator in the loop. The pioneering work on the haptic system stability is by Minsky et al. [5], where the discrete elements, the sampler and the hold, are approximated with continuous time models and Nyquist stability criterion is used to determine the stability of the overall system. In this paper, the human operator is approximated by a second order linear dynamical system. This approach later found use in many papers of the haptics literature such as in [6] Gillespie adopted a similar approach in modeling the human operator and analyzed the stability of the system. It has been shown that, the switching controller nature of the virtual wall and its discrete time implementation cause energy leaks and eventually this leakage may lead to instability. Like the early literature, more recent studies also use stability analysis methods to understand the effects of various different aspects of a haptic system. In [7], the uncoupled stability of the haptic system, where the human operator is not attached to the robot, is analyzed using the Routh-Hurwitz criteria to decide on the stability. This analysis is continued in [8–10], where the effects of physical damping, time delay, human operator on stability are investigated. A Lyapunov based approach to determine the stability of the haptic system is introduced in [11], where the effects of discretization, quantization, time delay and Coulomb friction on the stability of the haptic system are considered. It has been shown that achieving a passive haptic system is a hard task to achieve, especially in the presence of many deteriorating effects acting on the system. It has been shown that Coulomb friction allows the suppression of the high frequency oscillations in the haptic system. Moreover, this friction is beneficial for the safe operation of haptic systems with parameters violating the passivity condition.

Including the human operator model to the stability analysis or checking the uncoupled stability using classical linear control methods lead to a good understanding of the

effect of several parameters on stability; however, these approaches are not very suitable for implementation since they do not result in robust stability of the haptic system. Another branch of stability analysis is concerned with methods that rely on a large set of human operator models that satisfy certain conditions. Passivity assumption for human operator is one such approach and will be covered next.

Including the human operator model to the stability analysis or checking the uncoupled stability using classical linear control methods lead to a good understanding of the effect of several parameters on stability; however, these approaches are not very suitable for implementation since they do not result in robust stability of the haptic system. Another branch of stability analysis is concerned with methods that do not require detailed human operator. In this approach, the stability is considered for all possible human models under certain assumptions. The pioneering method in this branch is the passivity analysis. The passivity based methods assume that the human operator behaves as a passive element. This assumption is verified in [12], where it has been shown that within the frequency range required for the haptic applications, the human operator generally acts as a passive network element. In the field of teleoperation, the passivity is first applied by Anderson and Spong [13], where the analysis is performed for continuous time systems. Later, in his seminal work, Colgate introduced the passivity theorem for sampled-data systems and applied it to haptics [14]. Without requiring a human model, the overall haptic system is made passive such that the instabilities that may occur are avoided. This analysis made a huge impact since it handles the haptic system as a sampled-data system. However; this approach relies on the model of the virtual environment, which may not be available or may be too complex. In this case, the passivity of the haptic system cannot be guaranteed. The solution to this problem is also provided by Colgate through the concept of virtual coupling [15]. A virtual coupling acts as a buffer between the virtual environment and the robot; moreover, the coupler is designed such that the robot-coupler two-port network is always passive. The

overall system will stay passive if the two-port network is terminated with a passive human and a passive virtual environment. The virtual coupler idea is further extended in [16] to allow for admittance type devices. In this paper, Llewellyn's passivity theorem for two-port networks is used to result in less conservative conditions. In [17], energy bounding algorithm is introduced for haptic systems. This control approach satisfies robust passivity of the overall haptic system regardless of the damping frequency. The idea of this control method is to restrict the energy of the sample and hold devices such that it can be dissipated by the damping elements in the haptic system.

Passivity is not the only robust stability approach used in the haptics and teleoperation. In [18] μ-synthesis and H_∞ control techniques are applied to a bilateral teleoperation. The important aspect of these methods is that they do not require an assumption on the passivity of the human operator. Similarly, in [19], H_∞ control technique is applied to a bilateral teleoperation.

2.2 Transparency of Haptic Systems

The design problems in haptics is not limited to stability, transparency which is a measure of the effectiveness of the rendering, also presents a challenge. Stability is an indispensable aspect of a haptic system; however, it has been observed that robust stability conflicts with ideal transparency. In a teleoperation system, this conflict is analyzed by Lawrence in [20]. In haptics literature, a formulation of the relation between transparency and stability is provided in [16]. Hirche [21] investigated the transparency of the haptic system with constant time delay in the communication line. Griffits et al. analyzed the robust stability-trade-off in [22, 23]. They emphasize that better transparency can only be achieved through the violation of the passivity. This relation is metaphorically explained as the waterbed effect: an increase in one aspect is achieved by degrading the other.

The transparency of the system is measured by comparing the impedance felt by

the operator to the ideal impedance which should be felt. Mehling et al. introduced the concept of effective damping in [24]. Later, in [25], Colonnese et al. elaborated the idea to form a concrete transparency analysis method for all impedance types. The analysis method investigates the closed-loop impedance of the haptic system and culls the impedance transfer function into its real and imaginary parts. Together with the phase of the transfer function, those real and imaginary parts are the reflections of the rendered stiffness, damping or mass of the haptic system. Hence, the transparency of the haptic system can be revealed by comparing the rendered stiffness to the ideal case.

An inevitable reason of the loss of transparency is the impedance of the robot itself. In an ideal world, the human operator should only feel the impedance of the virtual environment; however, the physical existence of the robot is a source of distortion to haptic rendering. In reality, the human operator not only feels the virtual environment, but also the impedance of the robot is felt. To minimize this deficiency, a line of research focuses on the mechanical design of the haptic displays. In [26], Global Isotropy Index (GII) is introduced as a performance metric. In this method, the robot parameters are chosen such that the Jacobian of the robot exhibits an isotropic behaviour in the dexterous workspace. Later in [27], formed a framework based on the multicriteria optimization method called Normal Boundary Intersection (NBI) is used to simultaneously optimize the parameters of the haptic display for more than one design criteria. In [28], multicriteria optimization of parallel mechanisms is also considered. This design framework optimizes the dexterity, actuator utilization, uniformity over the workspace of the mechanism and the optimization problem is carried out by using the weighted sum of the objective functions and solving it with gradient based optimization routines. Finally, the feasibility of the solution is tested. In case of an abnormality in the optimal solution, the design procedure is reloaded with new weights on the objective functions.

Not all researchers handle the stability-transparency problem from mechanical design point of view. A pragmatic solution to this problem is introduced by Hannaford

and Ryu in [29]. The idea is to use an observer, named the passivity observer (PO), to trace the changes in the energy in and out of the system. If the energy is increasing, the controller, named the passivity controller (PC), supplies enough damping to the system. With this idea, instead of intervening to the system all the time, the controller takes action when it is necessary. Later, the idea of PO/PC is utilized in different control algorithms for haptics systems [29, 30]. Another approach for improving the transparency of the haptic system with robust stability is loop-shaping control introduced in [31]. In this approach, the human, robot and environment structure is reshaped into a form where only one feedback loop is available. Then, the standard frequency domain control design techniques are used to achieve robust stability with improved transparency. Loop-shaping approach is also utilized in [32], where it has been emphasized that the passivity of the human is a very restrictive condition. In order to provide less conservative results, a nominal model with an uncertainty bound is utilized for the human. The stability of the haptic system with this uncertainty is analyzed using the small gain theorem. In [33], Haddadi and Hastrudi-Zaad offered a different approach to the passivity vs transparency trade-off. Instead of considering an unbounded impedance range for the human operator, which is known to yield conservative results, they considered the absolute stability of a human operator with a bounded impedance and an environment with an unbounded impedance range. Their method is intuitive as it assumes a graphical representation.

2.3 Fractional Order Control

The name fractional is restrictive and misleading since the actual fractional order calculus deals with differentiation/integration of real or complex orders; however, due to historical reasons, this branch of mathematics is referred as fractional order calculus. Fraction order calculus is almost as old as the well know calculus of Newton and Leibniz. The letters between Leibniz and Bernoulli have the traces of the idea of differentiating

functions to fractional orders.

Fractional order calculus had long sought for an application and surprisingly enough that, the nature has provided the application for this interesting mathematical phenomenon. Viscoleastic materials, which are frequently seen in the nature, are exhibiting properties from elastic and viscous materials at the same time and they can be effectively modeled using fractional order calculus. With fractional order models, viscoelastic materials like lung or brain tissue of mammals can be represented with models which are capturing the true nature better than integer order models. For instance, in the literature, many papers on modeling such viscoelastic material with high order linear models, i.e. using mass-spring-damper elements, can be found. However, it has been noticed that, such an approach may not be capable of capturing the true nature of the system, and the use of fractional order calculus may lead to more capable models. In particular, it has been shown that using fractional order models can greatly reduce the degree of the model [34].

Fractional order control has also found extensive use in the robotics and control areas. A fractional order controller, called CRONE, is designed to exhibit isodamping behavior, even when the parameters of the system is changed [35]. A fractional order counterpart of the infamous PID controller is proposed in [36]. Tilted integral derivative (TID) is another fractional calculus based controller [37]. A quantitative comparison of these controllers are presented in [38]. Fractional order controllers are most commonly preferred in the motion control systems [39] due to their robustness. However, their application is not restricted to motion control; the fractional order control approaches has also been applied to position-force hybrid control in [40].

There are many notable books on fractional order control such as [41–45]. Also many tutorial and review papers are available [46–50].

CHAPTER III

PRELIMINARIES

In this chapter, the reader can find the preliminary information for the upcoming analyses. The haptic display, fractional order control, nondimensionalization of the haptic system parameters, virtual environment model with its characterization and, finally the, related passivity theorems are introduced in this chapter.

3.1 Haptic System

Figure 3.1 presents the block diagram of the haptic system in a sampled-data form. The human operator is represented with, possibly nonlinear, model $\phi(s)$ and an exogenous force $F_h^*(s)$. $G_r(s)$ denotes the haptic display. The feedback signal is chosen as the position measurements from the robot and is sampled with a time period of T. $H(z)$ represents the model of the virtual environment which is implemented on a digital computer. Finally, the computed reaction force, $F_e(z)$ passes through a zero-order hold and it is fed back to the plant.

The rigid body model of the haptic interface is shown in Fig. 3.2 and it is mathematically represented by $G_r(s)$, with m_r and b_r denoting the physical mass and viscous damping of the robot. For simplicity of the analysis, it is assumed that the human operator firmly grasps the robot; hence, $x_h = x_r$. Under these conditions, the equations of motion for the robot can be given as

$$m_r\ddot{x}_h + b_r\dot{x}_h = f_h + f_e \tag{3.1}$$

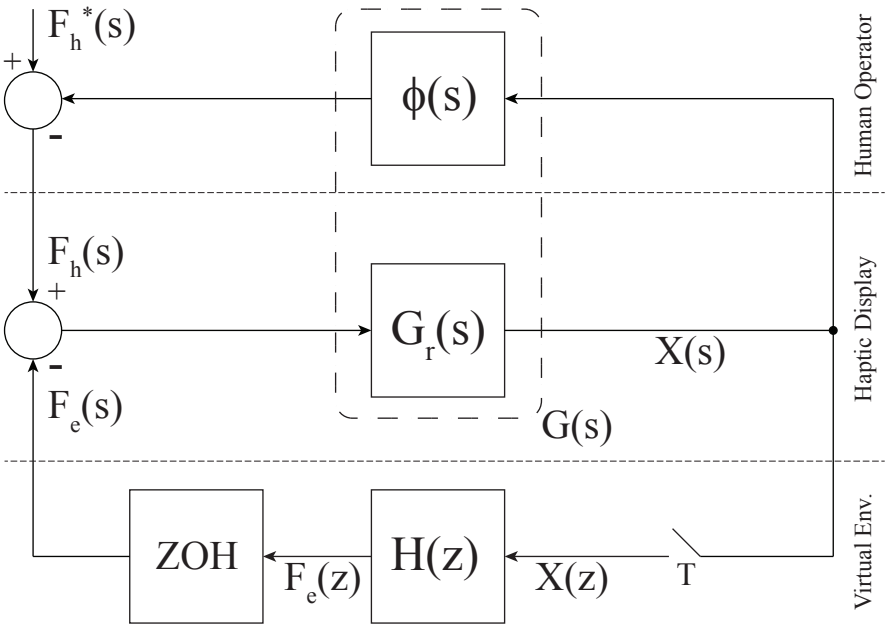

Figure 3.1: The sampled-data haptic system with ideal sampler and zero order hold.

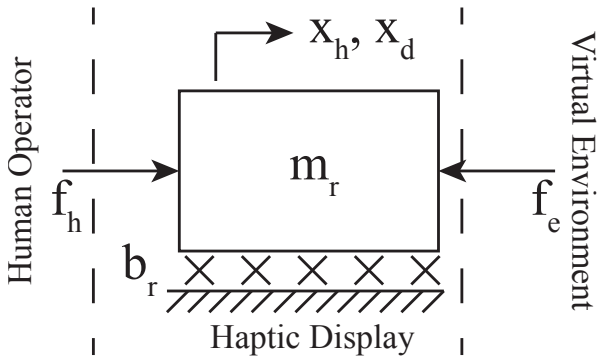

Figure 3.2: The model of the haptic interface

The corresponding transfer function of the haptic display from force to velocity in continuous time is

$$G_r(s) = \frac{1}{m_r s^2 + b_r s} \tag{3.2}$$

For the coupled stability analysis, the model of the human operator is necessary; however, an accurate model for human operator is generally non-linear, time varying and requires tedious experimentation for each individual. On the other hand, a simple LTI mass-spring-damper model is known to be sufficient for studying the main effects

of the presence of a human in the control loop. Therefore, the following second order linear model is adapted for the human operator.

$$\phi(s) = m_h s^2 + b_h s + k_h \tag{3.3}$$

If the sampled-data architecture is manipulated for combining the human and robot models, the following resulting transfer function can be obtained.

$$G(s) = \frac{1}{\underbrace{(m_h + m_r)}_{m} s^2 + \underbrace{(b_h + b_r)}_{b} s + \underbrace{k_h}_{k}} \tag{3.4}$$

3.2 Fractional Order Control

A general understanding of fractional order differointegrals and their properties is important in order to understand the realization of the control approach on a physical system. An operator for differointegration can be defined as follows

$${}_a\mathcal{D}_t^{\mu} = \begin{cases} \frac{d^{\mu}}{dt^{\mu}} & \mu > 0 \\ 1 & \mu = 0 \\ \int_a^t (dt)^{-\mu} & \mu < 0 \end{cases}$$

a is the initial time, t is the time and μ represents the differentiation order.
In the literature, many definitions of fractional order differointegrals exits. The most frequently used definitions are the Grunwald-Letnikov, Riemann-Liouville and Caputo's definitions. Riemann-Liouville is the most frequently used definition and is defined as

$${}_a\mathcal{D}_t^{\mu} f(t) = \frac{1}{\Gamma(n-\mu)} \frac{d^n}{dt^n} \int_a^t \frac{f(\tau)}{(t-\tau)^{\mu-n+1}} d\tau$$

where $n - 1 < \mu < n$ with $n \in \mathbb{Z}$ and Γ represents the gamma function.

Grunwald-Letnikov differointegral definition is important since it forms a basis for

the discrete implementation.

$$ {}_a\mathcal{D}_t^{\mu} f(t) = \lim_{h \to \infty} h^{-\mu} \sum_{j=0}^{\left[\frac{t-a}{h}\right]} (-1)^j \binom{\mu}{j} f(t - jh) $$

where [.] indicates the integer part of the real number, h is the step length for the differentiation.

Despite the frequent use of the previous definitions, in control systems, Caputo's definition is preferred, since handling of the initial conditions is more intuitive with this definition.

$$ {}_a\mathcal{D}_t^{\mu} f(t) = \frac{1}{\Gamma(n-\mu)} \int_a^t \frac{f^{(n)}(\tau)}{(t-\tau)^{\mu-n+1}} d\tau $$

for $n - 1 < \mu < n$ with $n \in \mathbb{Z}$ and Γ represents the gamma function. The analysis in this dissertation implicitly uses the Caputo's definition, since, this definition allows to define the initial conditions in terms of integer order derivatives.

For completeness, the properties of fractional order differointegral operator are summarized in the following list.

- The fractional order differointegral is a linear operator.

$$ {}_a\mathcal{D}_t^{\mu}(f(t) + g(t)) =_a \mathcal{D}_t^{\mu} f(t) +_a \mathcal{D}_t^{\mu} g(t) $$

- The fractional differointegral operator is causal. Assume $f(t) = 0$ for $t < 0$, then ${}_a\mathcal{D}_t^{\mu} f(t) = 0$.

- The fractional differointegral operator is shift invariant.

$$ {}_a\mathcal{D}_t^{\mu} f(t - t_0) =_a \mathcal{D}_t^{\mu} f(\tau)|_{\tau = t - t_0} $$

- If $f(t)$ is an analytic function of t, then its derivative is also analytic in both t and μ, where μ is the order of differentiation.

- For $\mu \in \mathbb{Z}$, the result of the fractional order derivative operator is same as the integer order one.

- Fractional order differointegral operator has semi-group property.

$$ {}_a\mathcal{D}_t^{\mu} f(t)\ {}_a\mathcal{D}_t^{\beta} f(t) = {}_a\mathcal{D}_t^{\beta} f(t)\ {}_a\mathcal{D}_t^{\mu} f(t) =_a \mathcal{D}_t^{\mu+\beta} f(t) $$

- Using the Caputo's definition, the Laplace transform is defined as

$$ \mathcal{L}({}_a\mathcal{D}_t^{\mu} f(t)) = s^{\mu}\mathcal{L}(f(t)) $$

The Caputo's definition allows defining initial conditions in terms of integer order derivatives; hence, for the final property, the initial conditions are defined in terms of integer order derivatives and they are assumed to be zero.

Note that, according to all definitions, the differointegration is a nonlocal phenomena and history-dependent. Computation of fractional order derivative includes a trade-off between the accuracy and computational speed. The accuracy increases as more data is used from the history to compute the current value of the derivative. However, depending on history heavily increases the computational burden. On the other hand, less history dependence can bring lesser computational burden with a loss in the accuracy. Even thought the trade-off is inevitable, the history dependence of the fractional order derivative decreases exponentially as we go further into the history. Therefore, with a high sampling rate, fractional order derivative can be assumed as history independent. This idea is named as the short memory principle and through out this dissertation, we adopt the short memory principle.

Even though it is possible to synthesize fractional order circuit elements to implement fractional order controllers in continuous time [52], the more common implementation methods is in discrete time through emulation. Discretization of fractional order system has attracted much attention in the literature and the existing approaches can be loosely categorized into two: The first approach is direct discretization, where the

exact mathematical model of the fractional order differointegral is used for further analysis. These direct discretization methods generally consider series expansions, such as MacLaurin series expansion, power series expansion, and continued fraction expansion. In [53], direct discretization is analyzed and polynomial approximations for arbitrary order differintegration is introduced. For the indirect method, a mathematical model is fitted to the frequency domain response of the fractional order differointegral. In [54], a two step approach to discretization is adopted. First, a frequency domain fit in continuous time domain is applied. Second, the continuous fit is discretized. In [55], a second order IIR differentiator based on Simpson Integration rule is presented. This method utilized a different calculation scheme of the transformation from s- to z-domain. In [56], least-squares based rational approximation of fractional order differointegrators is investigated. Details of different discretization schemes can be found in [48, 57].

The discretization scheme used in this paper can be summarized as follows. The discretization of the continuous transfer function is conducted via backward difference. Hence the fractional order differointegration becomes

$$s^{\mu} \rightarrow \left(\frac{1 - z^{-1}}{T} \right)^{\mu} \tag{3.5}$$

where, without loss of generality, $\mu \in [-1, 1]$. The discrete fractional differointegrator can be approximated by the following recursion.

$$(1 - z^{-1})^{\mu} = A_n(z^{-1}, \mu) \tag{3.6}$$

where n is the order of the approximation and the recursion rule is

$$A_n(z^{-1}, \mu) = A_{n-1}(z^{-1}, \mu) - c_n z^n A_{n-1}(z, \mu) \tag{3.7}$$

$$c_n = \begin{cases} \mu/n, & \text{n is odd} \\ 0, & \text{n is even} \end{cases}$$

For further details of fractional order calculus and the discrete time implementation

of fractional order model, the reader is referred to [43, 46, 58].

3.3 Virtual Environment

As presented in Fig. 3.1, in a typical haptic system, the virtual environment is implemented in discrete time and connected to the physical (continuous time) robot via sample and hold mechanisms. This implementation method leads to a great flexibility in creating virtual environments of arbitrary complexity, while the mathematical analysis of the system require more sophisticated tools.

The aim of this study is to investigate the effect of using fractional order dynamics in the virtual environment. Therefore, among many possibilities, a simple virtual environment model consisting of an elastic and a fractional order damping elements are chosen, due to the capability of this model on revealing the effects of fractional order dynamics on the system performance, while preserving an acceptable level of simplicity in the calculations. This environment model is given in Eq. 3.8.

$$H(z) = K + B\left(\frac{1 - z^{-1}}{T}\right)^{\mu} \qquad \mu \in [0, 2] \tag{3.8}$$

In this virtual environment model, K and B are respectively the linear virtual stiffness and the fractional order dissipation element parameters. It is important to note that in this virtual environment model, the order of the differentiator is not necessarily an integer number. The analysis is conducted for $\mu \in [0, 2]$, where $\mu = 1$ corresponds to the classical first order backward difference differentiator. We also consider only the positive values of K and B. Throughout the analysis, the velocity of the robot is approximated using the backward difference method. Although different velocity approximation methods can be employed for discrete time implementations of the virtual environment, the finite difference approach is preferred due to its simplicity. Moreover, since this approach has been extensively used in the literature, this choice enables a comparison of the performance between the integer and fractional order models.

3.4 Nondimensionalization of the System Parameters

Nondimensional parameters are adapted for the analysis, since as the differentiation order changes, the physical meaning, as well as the unit of B changes. Nondimensional parameters enable comparison of virtual environment models with different differential orders. The nondimensionalization is achieved through the following transformations. Note that these transformations extend the ones noted in [8] with the generalized dissipation element. In particular, we define the nondimensionalization of virtual damping to fractional order dissipative elements as follows

$$\begin{aligned} K \ \rightarrow \ \alpha = \frac{KT^2}{m}, \quad B \ \rightarrow \ \beta = \frac{BT^{2-\mu}}{m}, \\ b \ \rightarrow \ \delta = \frac{bT}{m}, \qquad k \ \rightarrow \ \gamma = \frac{kT^2}{m} \end{aligned} \tag{3.9}$$

3.5 Characterization of the Virtual Environment

Understanding the behaviour of a virtual environment with fractional order element is not a trivial process since a consensus on clear visualization of the fractional order derivative is not available. Therefore, before delving into the stability characteristics, effective impedance analysis, which reflects the frequency dependent behaviour of an impedance, is provided. The use of effective impedance analysis in haptics is proposed in [24, 25]. This analysis not only reveals how a fractional order virtual wall behaves in the frequency range up to the Nyquist frequency, but also may help decide on a proper differentiation order for a given task.

In order to perform the effective impedance analysis on the virtual environment with fractional order model, the definitions of effective stiffness (ES) and effective damping (ED) are adjusted for position feedback as

$$ES(\omega) = \Re^{+}\{H(e^{j\omega T})\} \tag{3.10}$$

$$ED(\omega) = \frac{1}{\omega}\Im^{+}\{H(e^{j\omega T})\} \tag{3.11}$$

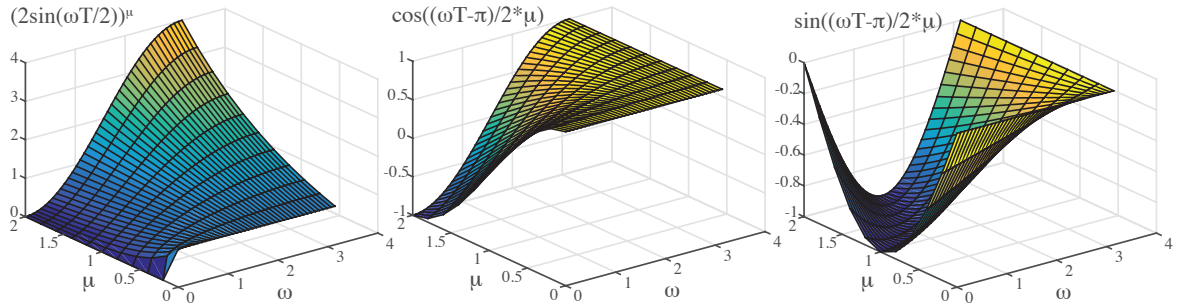

Figure 3.3: Coefficients that scale effective stiffness and damping of the fractional order virtual environment

For the virtual wall model given in Eq. 3.8, the effective stiffness and damping are read as

$$ES(\omega) = K + B\left(2\sin\frac{\omega T}{2}\right)^{\mu}\cos\left(\frac{\omega T-\pi}{2}\mu\right) \tag{3.12}$$

$$ED(\omega) = \quad -B\left(2\sin\frac{\omega T}{2}\right)^{\mu}\sin\left(\frac{\omega T-\pi}{2}\mu\right) \tag{3.13}$$

Note that $-\pi/2 \leq (\omega T-\pi)/2 \leq 0$ lives in the fourth quadrant; hence, for $0 \leq \mu \leq 1$, $(\omega T-\pi)\mu/2$ is always in the fourth quadrant, while for $1 \leq \mu \leq 2$, $(\omega T-\pi)\mu/2$ can lie in the third or the fourth quadrants.

Fractional order models can also significantly affect the transparency aspects of a haptic system. In particular, in Section 3.5 we have presented expressions for calculating effective impedance of discrete time fractional virtual environments, since this analysis is effective in revealing the frequency dependent behaviour of fractional order impedances. Fig. 3.3 depicts the three frequency dependent coefficients in Eq. 6.1 and 6.2 that shape the response of effective spring and damping terms.

In Eq. 6.1 characterizing the effective stiffness, α is a positive number, always contributing positively to the effective stiffness. On the other hand, effective stiffness also has a β dependent term that can increase or decrease its value as a continuous function of ω and μ. If $0 \leq \mu \leq 1$, cosine term in Eq. 6.1 is always positive, independent of ω; hence, the contribution of β on the effective stiffness is always positive. However, if $1 \leq \mu \leq 2$, then the cosine term can change sign; therefore, depending of the frequency,

the effective stiffness can also be lowered.

In Eq. 6.2 characterizing the effective damping, as expected, one can observe that there is no contribution of μ. Effective damping should always be positive, and this is indeed the case, since $\sin\left(\frac{\omega T-\pi}{2}\mu\right)$ is always in third or fourth quadrants. As a result for $\alpha \in (0,2)$, the effective damping is positive and there is dissipation in the system. The magnitude of the effective damping is predominantly determined by $(2\sin(\omega T/2))^{\mu}$ term and by choosing $1 \leq \mu \leq 2$ the effective damping can be increased significantly at high frequencies, compared to $0 \leq \mu \leq 1$.

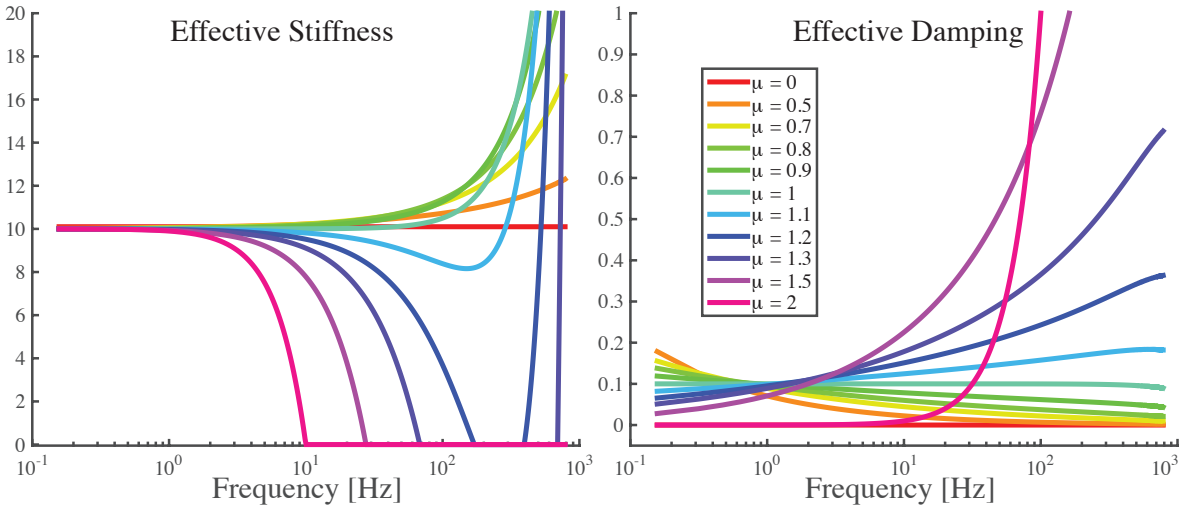

Figure 3.4: Effective stiffness and damping of the fractional order virtual environment of Eq. 3.8.

Fig. 3.4 depicts the effective stiffness and damping of a sample fractional order virtual environment with $K = 10$ N/mm, $B = 0.1$ Ns/mm and $T = 0.001$ s. From the figure, the frequency and differointegration order dependence of the effective stiffness and damping can be observed. Noting the frequency separation between human input and noise, differointegration order can be put in good use to adjust the frequency characteristics of effective impedance such that good transparency behavior can be ensured within the human bandwidth, while better stability robustness is achieved at higher frequencies.

After visualizing the virtual environment with fractional order elements, we are

ready to characterize the stability of the overall haptic.

3.6 Passivity of Haptic System

Passivity, as explained in the previous chapter, is an important tool in the stability analysis of haptic systems. In the literature, there are two branches for analyzing the passivity of a haptic system. In the first approach, the haptic display and the virtual environment are handled together and passivity analysis is conducted such that the virtual environment parameters do not cause an active behavior for the overall system. In this approach, the knowledge of the exact model of the virtual environment is crucial. The second approach assumes that the implemented virtual environment has passive dynamics, i.e. it does not generate energy and a virtual coupler, explained in the upcoming sections, is attached to the haptic display where the combined system can be represented as a two port network. The virtual coupler is designed such that the overall two port network stays passive.

3.6.1 Haptic System in One Port Network Form

The passivity analysis of a haptic display is first analyzed in [59]. Later in [60] the passivity condition is formalized. Since the analysis of this paper relies on this theorem, the theorem is repeated from [14]. The network representation of this approach can be seen in Fig. 3.5.

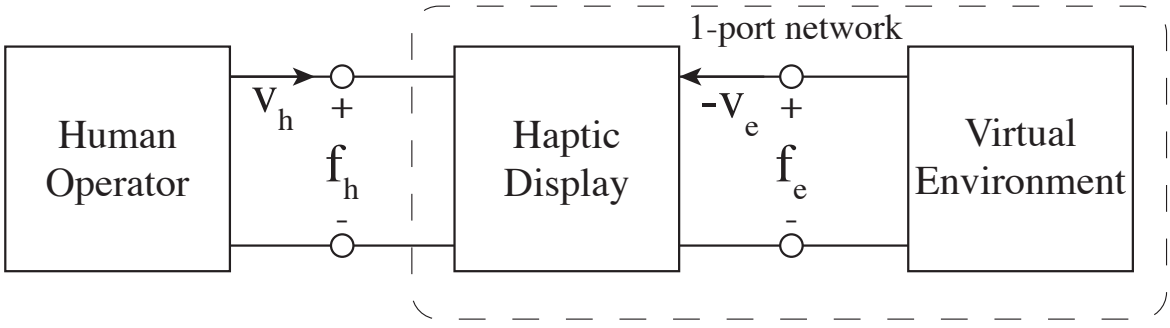

Figure 3.5: One port network representation of a haptic system

Theorem 1 (Passivity of a haptic interface [14]). *A necessary and sufficient condition for the passivity of the haptic interface model in Figure 3.1 is*

$$b > \frac{T}{2}\frac{1}{1-\cos(\omega T)} Re\left\{\left(1-e^{-j\omega T}\right) H(e^{j\omega T})\right\} \tag{3.14}$$

for $0 \leq \omega \leq \omega_N$, *where* $\omega_N = \pi/T$ *is the Nyquist frequency.*

3.6.2 Haptic Systems in Two Port Network Form

Handling the haptic system as a two port network is first accomplished in [15]. This approach, especially, important for handling virtual environments with complex dynamics or for the case when a clear model of the virtual environment is missing. The important step in this approach is the introduction of the virtual coupler which acts as a buffer between the haptic display and the virtual environment. An illustration of this method can be seen in Fig. 3.6

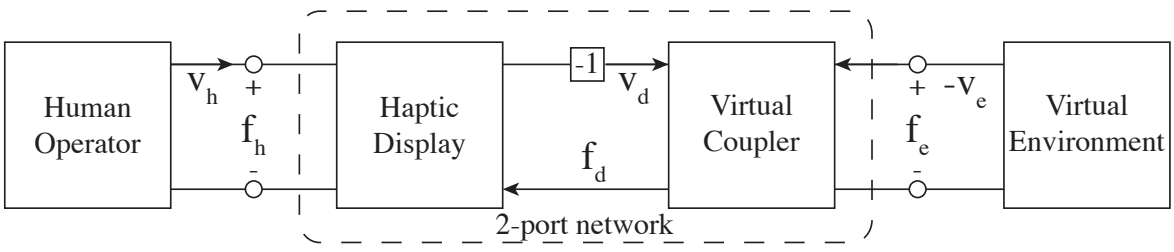

Figure 3.6: Two port network representation of a haptic system with virtual coupling

The passivity of such systems can be check by Llewellyn's absolute stability criteria.

Definition 1. *The necessary and sufficient conditions for a 2-port network to be absolutely stable are*

$$\begin{aligned} \Re\{p_{11}\} &\geq 0 \\ \Re\{p_{22}\} &\geq 0 \\ 2\Re\{p_{11}\}\Re p_{22} &\geq |p_{12}p_{21}| + \Re\{p_{12}p_{21}\}, \quad \forall\omega \geq 0 \end{aligned}$$

CHAPTER IV

STABILITY ANALYSIS AND EXPERIMENTAL VERIFICATION

In this chapter, the discrete-time stability analysis for the haptic system is conducted.

4.1 Discrete-Time Transfer Functions

Discrete domain is chosen for the analysis and zero-order-hold (ZOH) equivalent representation is preferred, since the real-time implementation of a haptic system is usually carried out using ZOH circuits. The ZOH equivalent discrete time counterpart of continuous time system (3.4) with nondimensional parameters becomes

$$\begin{aligned} G(z) =& \frac{T^2}{m} \frac{((2-c_2-c_3)c_1+(c_2-c_3)\delta)z}{2c_1\gamma(z^2-(c_2+c_3)z+e^{-\delta})} \cdots \\ &+ \frac{(2e^{-\delta}-c_3-c_2)c_1+(c_3-c_2)\delta}{2c_1\gamma(z^2-(c_2+c_3)z+e^{-\delta})} \end{aligned} \tag{4.1}$$

where $c_1 = \sqrt{\delta^2-4\gamma}$, $c_2 = e^{-(\delta+c_1)/2}$, $c_2 = e^{-(\delta-c_1)/2}$.

In order to perform a stability analysis on the fractional order transfer function, we adopt one of the existing discretization schemes to represent the fractional order elements in terms of their integer order equivalents. Among many well-performing methods, the direct method of Muir recursion introduced in [53] is adopted for the rest of the paper. In particular, the third order polynomial approximation is chosen so that the degree of the differentiator can be kept low, while the approximation error is relatively low. Using this discretization scheme, the fractional order virtual environment

model can be written in the discrete form as

$$H(z) = K + B\frac{-\frac{1}{3}\mu z^{-3} + \frac{1}{3}\mu^2 z^{-2} - \mu z^{-1} + 1}{T^{\mu}} \tag{4.2}$$

Using Eq. 3.9, the nondimensional form of the virtual environment can be given as

$$H(z) = \frac{m}{T^2}\left(\alpha + \beta\left(-\frac{1}{3}\mu z^{-3} + \frac{1}{3}\mu^2 z^{-2} - \mu z^{-1} + 1\right)\right) \tag{4.3}$$

Finally, the overall transfer function of the discrete-time system from the exogenous human force to position output of the robot is given by

$$G_x(z) = \frac{G(z)}{1 + G(z)H(z)} \tag{4.4}$$

4.2 Stability Analysis

The stability analysis is conducted using the Routh-Hurwitz method. The characteristic polynomial of the closed-loop haptic system with human operator coupled to the haptic display can be found in the denominator of (4.4). Using bilinear transformation, $z \leftarrow (1+w)/(1-w)$, the discrete-time transfer function is transformed into the proper form for Routh-Hurwitz test. The stability of this new polynomial, which is in w-plane, implies the stability of the discrete-time characteristic polynomial in z-plane.

4.3 Stability Regions

The user imposes on the haptic system an impedance, consisting of stiffness, damping, and mass. Even though this impedance can change based on the user's grip, it typically contains relatively low stiffness and high damping [11]. One of the worst-case stability scenario takes place when there is minimal damping, during which the user is not or is barely touching the haptic device. Another worst-case condition occurs when the mass of the haptic display is minimal. In this case, the system is vulnerable to experience vibrations which are insufficiently filtered out due to the low mass of the robot.

One other worst-case scenario is the energy introduced by the human operator. However, it has between observed that human is getting well with passive physical objects [12]. Moreover, as it is stressed out in [11], human operator can operate about 10 Hz. Therefore, the energy injected to the system at this frequency can be well damped by the friction of the system.

A stronger user grip imposes additional damping and mass to the system, augmenting the natural damping of the device and may help with coupled stability. Hence, in practice, a light/no grip represents one of the most challenging case for stability analysis.

In this section, the stability of the close-loop haptic system is analyzed without involving a human operator, that is, when $m_h = 0$, $b_h = 0$ and $k_h = 0$ and only parameters of the robot (m_r and b_r) are utilized. This setup is useful, since it is easier to ensure repeatability of the experimental results. Furthermore, this set up can thoroughly reveal the effect of differentiation order, without complicating the results due to the involvement of the human operator.

Stability regions — the region in the α-β plane, where the closed-loop uncoupled haptic system stays stable — of uncoupled haptic device for various differentiation orders are presented in Fig. 4.1.

One can observe from Fig. 4.1 that, for $\mu \in (0, 2)$ the area under the stability region increases as the differentiation order of the virtual environment increases up $\mu = 2$. It is important to note that when $\mu = 2$, β corresponds to an ideal nondimensional kinetic energy storage (inertia) element and the highest stiffness rendering for the haptic device is achieved. This observation is in agreement with the analysis emphasized in [61] and as expected, the fractional order analysis can recover the results for the integer order case.

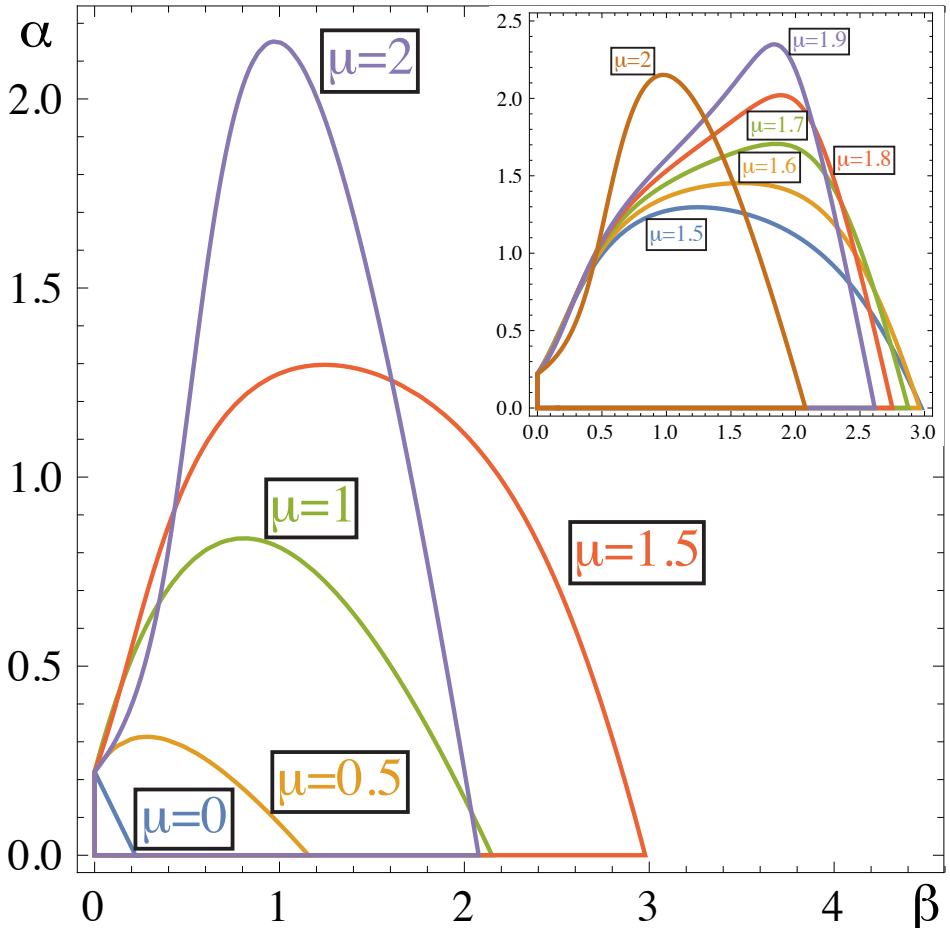

Figure 4.1: Stability region of haptic system for various differentiation orders

4.4 Testbed and Experiments

Experiments for the uncoupled stability of the haptic system is conducted on a single DoF voice coil actuated haptic display shown in Fig. 4.2. The apparent inertia of the robot is $m_r = 65$ g and its physical damping is characterized as $b_r = 3.5 \times 10^{-3}$ N s/mm.

The virtual environment is a fractional order wall located at the initial position of the end effector, so that there is no impact during the interaction of the robot with this virtual environment. During the experiments, the robot pushes the virtual wall with a constant force of 1 N and the parameters of the wall are changed until the interaction becomes unstable. The robot interacts with the virtual wall for 5 s and last 0.4 s period

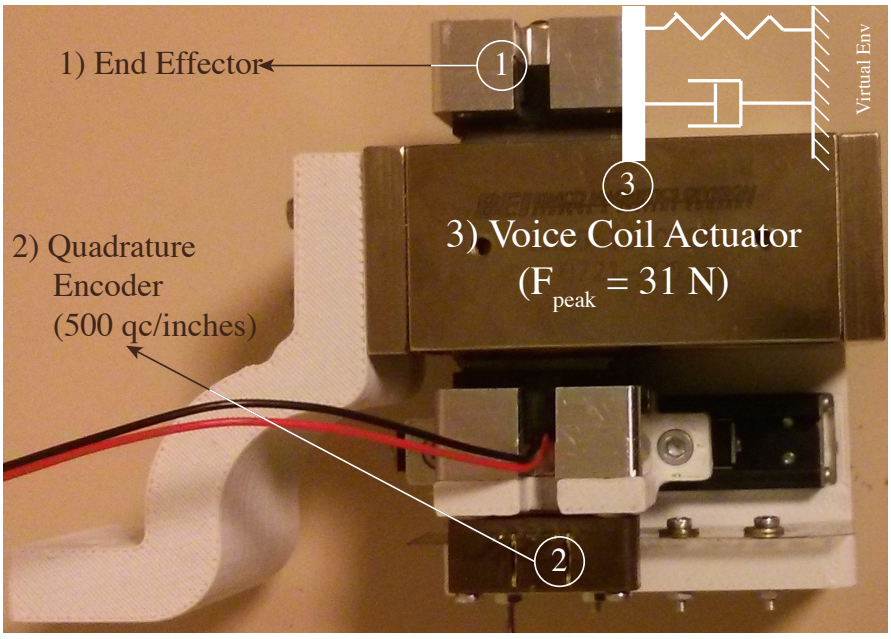

Figure 4.2: Single DoF voice coil actuated haptic display

of this interaction is considered for the analysis. The criteria for determining instability is chosen based on the standard deviation of the end effector position during the last 0.4 s of the interaction. If the standard deviation is greater than 0.1 mm, then the interaction marked as unstable. This threshold is determined empirically such that it prevents the end-effector to oscillate significantly, but it is not very conservative, allowing for very small amplitude oscillations. In the experiments the sampling time is set as $T = 0.002$ s.

Fig. 4.3 depicts the results for the Z-width experiments for the voice coil actuated experimental setup introduced in Fig. 4.2. The experiments are performed for $\mu \in \{0, 0.5, 1, 1.5, 2\}$, under the same conditions for which the theoretical analysis is conducted.

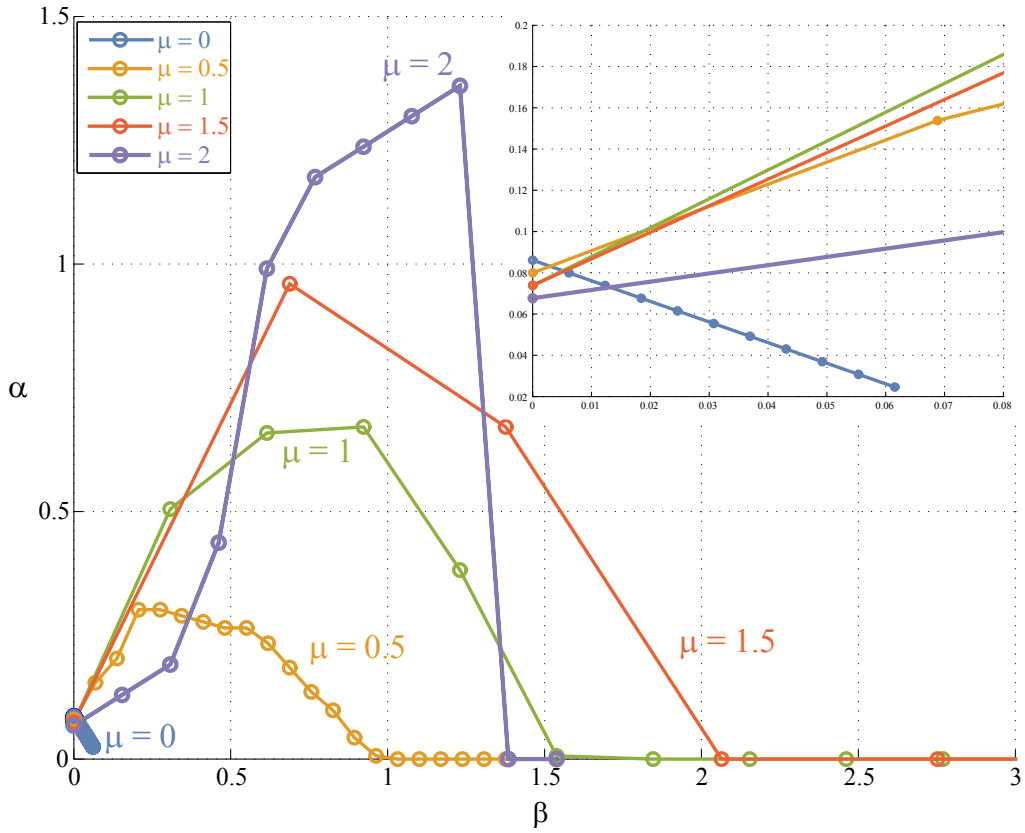

Figure 4.3: Results of Z-width experiments of the haptic system

4.5 Comparison

Comparison of theoretical results presented in Fig. 4.1 and experimental Z-width results depicted in Fig. 4.3 reveals that the experimental results indeed capture the effect of differentiation order on the stability region. In particular, as expected from the analysis, the stability region increases as the differentiation order increases. The highest stiffness rendering takes place at the differentiation order $\mu = 2$. The decrease in β during the transition from $\mu = 1.5$ to $\mu = 2$ is also captured by the experiments.

The experimental results successfully capture the qualitative relationship among different differentiation orders as predicted by the analysis. On the other hand, the results do not match quantitatively, due to unmodeled effects such as, quantization errors, uncertain system parameters, and higher order robot dynamics. Moreover, it can be observed that, as the differentiation order increases, the discrepancy between the

theoretical and experimental stability regions increases. This phenomena is, mainly, due to the intrinsic noise amplification property of digital derivative estimators. A thorough analysis of the noise amplification of fractional order differentiators can be found in [62].

4.6 Sensitivity of Stability Regions to Changes in Model Parameters

In this section, we analyse the effect of changes in parameters b, k and T on the stability regions, for different differentiation orders. For the analysis, we utilize the ZOH equivalent of the transfer function in (3.4) that consists of the coupled human and the robot model. Hence, the change in system parameters b and k can be considered as the effect of different users interacting with the device.

Fig. 4.4 presents a matrix of plots depicting stability regions for different differentiation orders μ, under changes in the non-dimensional parameters δ and γ.

The effect of varying the sampling time (T) Varying the sampling time (T) of the system affects both the non-dimensional damping δ and the non-dimensional stiffness γ parameters of the closed-loop system, such that increasing the sampling time T necessitates decreasing both δ and γ to ensure stability. One can observe from the first column of Fig. 4.4 that increasing T reduces the stability region of the closed-loop haptic system. This result is expected and similar to the integer order case, since the stability of sampled-data systems deteriorate as the sampling frequency decreases. However, the change in the stability region for a fixed change in T decreases significantly as the differentiation order μ increases. This observation indicates the robustness of fractional order systems to changes in T, as the differentiation order gets higher.

The effect of varying the dissipation parameter (b) Perturbations in b are directly proportional to perturbations in the non-dimensional parameter δ. One can observe from the second column of Fig. 4.4 that as the dissipation coefficient b (hence

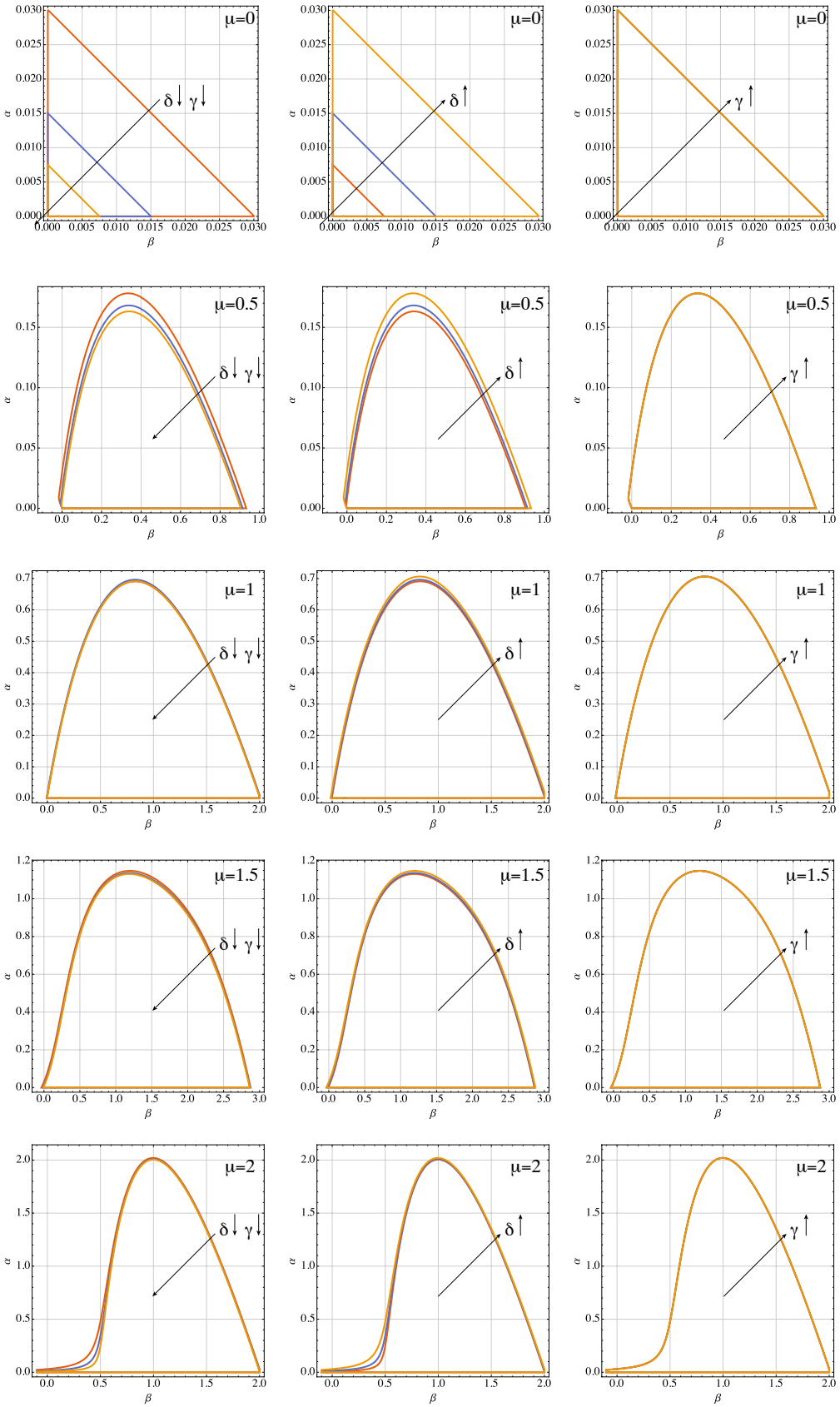

Figure 4.4: Stability regions for different differentiation orders, under changes in non-dimensional parameters δ and γ.

δ) is increased, the stability regions get larger. However, the change in the stability region for a fixed change in b decreases as the differentiation order μ increases. This observation indicates that as the differentiation order becomes higher, stability of the system becomes less dependant on the dissipation coefficient.

The effect of varying stiffness parameter (k) Perturbations in k are directly proportional to perturbations in the non-dimensional parameter γ. One can observe from the third column of Fig. 4.4 that changes in stiffness do not have a significant effect on the closed-loop stability of the coupled haptic system. This observation is independent from the order of differentiation. Note that a similar observation is noted in [8] for the integer order case. Our result generalizes this observation to fractional order systems.

4.7 Case Study

Fig. 4.5 presents the magnitude plot of the sensitivity function of the fractional order sample-data haptic system for different differentiation orders. One can observe from this figure that as the differentiation order μ gets smaller, the peak magnitude of the sensitivity function decreases, indicating that the system becomes more robust to parameter changes.

Fractional order transfer functions are commonly utilized in robust motion control literature to result in favorable frequency responses [35] since they allow for much larger range of frequency responses to be synthesized. Fig. 4.5 is an example of such a case, where decreasing the differentiation order results in favorable stability robustness for the given set of system parameters. In general, even though it is possible to make use of the extra degree of design freedom introduced by the fractional differentiation order into good use to achieve favourable system response, the effect of the fractional differentiation order on the system response is not trivial and strongly depend on system

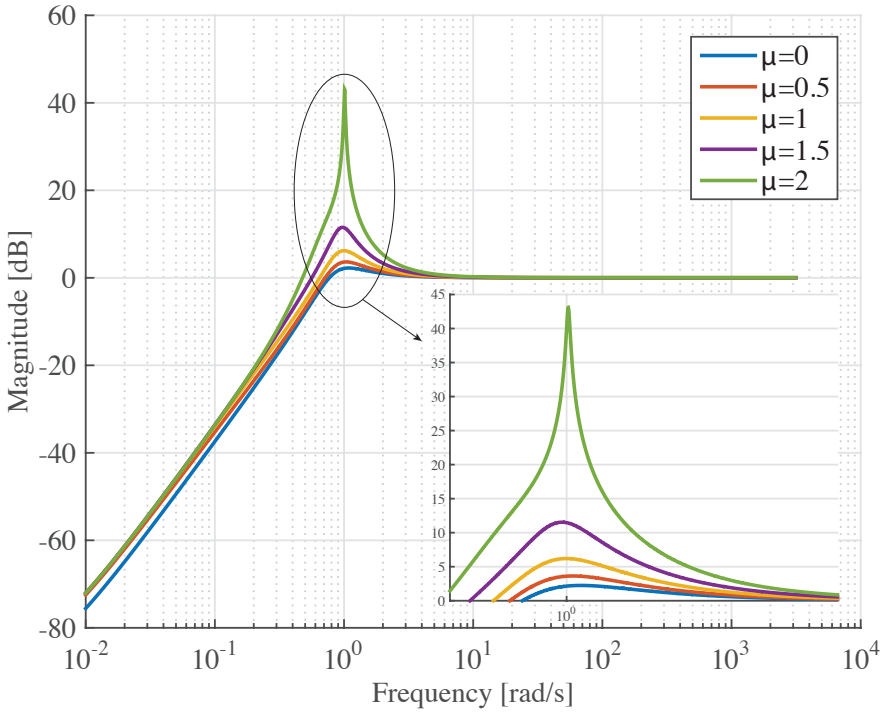

Figure 4.5: Sensitivity transfer function of the fractional order haptic system for different differentiation orders μ

parameters.

4.8 Discussion

For a haptic system with fractional order controller in its virtual environment, the differentiation order can be chosen considering the needs of the application at hand. If the transparency of the stiffness rendering is more important and there is enough damping in the system to ensure coupled stability, then the differentiation order can be preferred to be in the range $[0, 1]$. However, if the haptic system lacks physical damping, than energy dissipation due to the virtual damping in the controller becomes important and the differentiation order may be set to a value in the range $[1, 2]$ to amplify the effective damping of the system for higher frequencies. It is important to note that, the commonly used integer differentiation order of 1 presents a good compromise, since it both contributes to stiffness rendering and can supply considerable amount of damping.

However, before concluding the necessity of a fractional order environment model and discussing its effectiveness, we have to investigate effect of this new control method on the passivity and transparency characteristics of the overall haptic system.

4.9 Conclusions

We have proposed utilization of fractional order models/controllers in haptic systems and analyzed the stability of fractional order haptic systems. We have computed stability regions for systems with different orders and experimentally verified these results though a single DoF haptic interface. Our results indicate the non-dimensional stability region enlarges as the differentiation order is increased from 0 to 2. Furthermore, we have observed that fractional order system order can directly affect the stability robustness under parameter variations.

In general, the extra degree of design freedom introduced to the control system by the fractional differentiation order seems promising, since it allows one to better shape the frequency response of the system to achieve more favorable performance characteristics.

The second half of this dissertation focuses on the passivity characterization of haptic systems with fractional order dynamics in the virtual environment. Moreover, the fractional order control idea is expanded to control of haptic systems with virtual coupling. Finally, an application example based on fractional order control is presented.

CHAPTER V

PASSIVITY OF THE HAPTIC SYSTEM

As it has been pointed out, a stability analysis relying on a human operator model can be misleading for real world applications. This mislead is mostly hindering from the difficulties of fitting an appropriate model to the human operator.

The widely accepted solution of human modeling problem relies on passivity theory. In this theory, first and foremost assumption is that the human operator behaves as a passive element in the control network. With this assumption, a passive human operator driving, or in network theory jargon terminating, a passive haptic display with haptic controller, indicates a stable behaviour during the course of operation.

In case of complex environments, or in the absence of an environment model, passivity theory provides acceptable controllers. In these problems, one has to use virtual coupling, a controller placed between the haptic display and the virtual environment, and the aim of the controller design should be achieving a passive two port network, which consists of the haptic display and the virtual coupler. Hence, the overall system is passive if this passive two port network is terminated by passive one port networks which are the human operator and the virtual environment.

The rest of this chapter analyzes the passivity properties of fractional order controllers in haptic systems. In the first section, the passivity of a haptic system with a known, and simple, virtual environment model. The passivity analysis utilizes the infamous theorem of Colgate on the passivity of sampled-data systems. From a network theory point of view, this case corresponds to analyzing the passivity property of a one

port network.

The second passivity analysis is conducted for a haptic system where the human and the environment models are not available; however, they are assumed to be passive. In this analysis, the virtual coupler is contains fractional order dynamics and the passivity of the two port network, consisting of the haptic display and the fractional order virtual coupler is sought.

5.1 Haptic System in One Port Network Form

Corollary 1. *Consider a haptic system with a robot model as given in Eq. 3.2 and a virtual environment model as described in Eq. 3.8 inside the control architecture introduced in Fig. 3.1, where human is modeled as passive operator. For positive values of B and K, the overall system is passive if the following inequality is satisfied.*

$$b > \frac{KT}{2} + B\left(\frac{T}{2}\right)^{1-\mu} \tag{5.1}$$

The dimensionless form of Eq. 5.1 can be expressed as

$$\delta > \frac{\alpha}{2} + \beta\left(\frac{1}{2}\right)^{1-\mu} \tag{5.2}$$

where non-dimensionalization is performed according to Eq. 3.9.

Proof. Corollary 1 follows Theorem 1 in Section 3.1. In particular, let the branch cut for the analysis be chosen at $-\pi$ and consider the first Riemannian sheet, which is physically meaningful. Replace the virtual wall model of Eq. 3.14 with the virtual wall model of Eq. 3.8 to obtain

$$b > \frac{T/2}{1-\cos(\omega T)}\Re\left\{\left(1-e^{-j\omega T}\right)\left(K + B\left(\frac{1-e^{-j\omega T}}{T}\right)^{\mu}\right)\right\} \tag{5.3}$$

$$b > \frac{KT}{2} + \frac{BT^{1-\mu}}{2}\frac{\Re\left\{\left(1-e^{-j\omega T}\right)^{1+\mu}\right\}}{1-\cos(\omega T)} \tag{5.4}$$

Representing $1-e^{-j\omega T}$ in the phasor notation and substituting for $1-\cos\omega T$

$$1-e^{-j\omega T} = \sqrt{2(1-\cos\omega T)}\; e^{-j\frac{\omega T-\pi}{2}} \tag{5.5}$$

$$1-\cos\omega T = 2\sin^2\frac{\omega T}{2} \tag{5.6}$$

one can further manipulate the equations as follows

$$b > \frac{KT}{2} + \frac{BT^{1-\mu}}{2} \frac{\Re\left\{\left(\sqrt{2(1-\cos\omega T)}\, e^{-j\frac{\omega T-\pi}{2}}\right)^{1+\mu}\right\}}{2\sin^2\frac{\omega T}{2}} \tag{5.7}$$

$$b > \frac{KT}{2} + \frac{BT^{1-\mu}}{2} \frac{\left(\sqrt{4\sin^2\frac{\omega T}{2}}\right)^{1+\mu} \Re\left\{e^{-j\frac{\omega T-\pi}{2}(1+\mu)}\right\}}{2\sin^2\frac{\omega T}{2}} \tag{5.8}$$

$$b > \frac{KT}{2} + \frac{BT^{1-\mu}}{2} \frac{\left(2\sin\frac{\omega T}{2}\right)^{1+\mu} \cos\left(\frac{\omega T-\pi}{2}(1+\mu)\right)}{2\sin^2\frac{\omega T}{2}} \tag{5.9}$$

$$b > \frac{KT}{2} + B\left(\frac{T}{2}\right)^{1-\mu}\left(\sin\frac{\omega T}{2}\right)^{\mu-1}\cos\left(\frac{\omega T-\pi}{2}(1+\mu)\right) \tag{5.10}$$

The system is passive if Eq. 5.10 holds for all frequencies $0 \leq \omega \leq \pi/T$. In order to obtain Eq. 5.1, the worst-case scenario, or the maximum value of the frequency dependent part of the previous inequality, has to be determined, since B is known to be positive. Let the frequency dependent part of the inequality be represented as

$$f(\omega,\mu) = \left(\sin\frac{\omega T}{2}\right)^{\mu-1}\cos\left(\frac{\omega T-\pi}{2}(1+\mu)\right) \tag{5.11}$$

The extrema of this function occurs at frequencies where $\partial f(\omega,\mu)/\partial\omega = 0$. The first partial derivative of $f(\omega,\mu)$ with respect to ω can be expressed as

$$\begin{aligned}\frac{\partial f(\omega,\mu)}{\partial\omega} = -\left(\sin\frac{\omega T}{2}\right)^{\mu-1}\Bigg[&(1-\mu)\cot\frac{\omega T}{2}\cos\left(\frac{\omega T-\pi}{2}(1+\mu)\right)\ldots \\ &+ (1+\mu)\sin\left(\frac{\omega T-\pi}{2}(1+\mu)\right)\Bigg]\end{aligned} \tag{5.12}$$

After some manipulations, Eq.5.12 can be transformed into

$$\sin\left(\frac{\omega T-\pi}{2}\right) - \mu\sin\left(\omega T - \frac{\omega T-\pi}{2}\mu\right) = 0 \tag{5.13}$$

For an arbitrary μ, this equation holds if both sine terms are vanish and this condition occurs at $\omega = \pi/T$. Moreover, the second partial derivative of $f(\omega,\mu)$ with respect ω to is negative for $\omega = \pi/T$, ensuring that $\omega = \pi/T$ is where the function attains a maximum value. Closely investigating the 3D plot of $f(\omega,\mu)$ confirms that the global maximum is always attained at $\omega = \pi/T$, the Nyquist frequency of the sampled-data system. Substituting this value into Eq. 5.10 completes the proof. □

Remark 1. *Besides from the usual virtual wall parameters, K and B, fractional order controller introduces a new design parameter, μ, which can be set to any real number. The new parameter explicitly shows up in the passivity condition and introduces new opportunities to improve the overall performance of the haptic system. Fig. 5.1 depicts*

the solution of Eq. 5.1 for various values of μ.

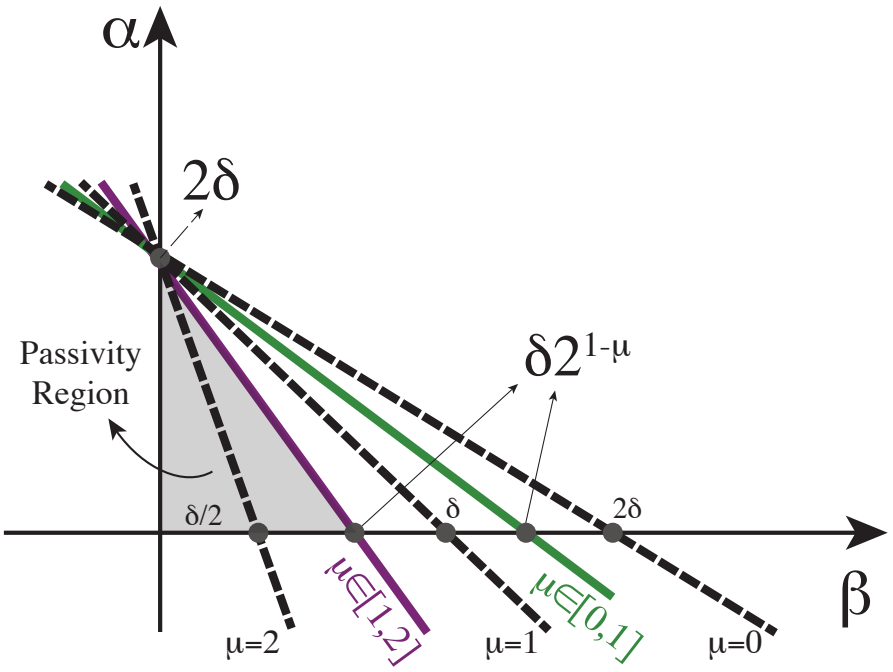

Figure 5.1: Nondimensional passivity regions for different values of differentiation order μ

Remark 2. *Eq. 5.1 is a generalization of the celebrated passivity condition for haptic systems, introduced by Colgate in [14], to the fractional order case. A close investigation reveals that, for $\mu = 1$, Eq. 5.1 can recover the familiar integer order condition. Moreover, the other integer order cases of $\mu = \{0, 2\}$ can also be easily recovered from Eq. 5.1.*

5.2 Haptic System in Two Port Network Form

The haptic interface is modeled as a rigid robot and it is assumed that the human operator firmly grasps the robot; hence, $x_h = x_r$. The 2-port analysis in this dissertation closely follows the one in [16]. The analysis is conducted in discrete-time and the continuous models are transformed to discrete-time domain using Tustin's approximation. The impedance of the is given as

$$Z_d(z) = ms + b|_{s \leftarrow \frac{2}{T}\frac{z-1}{z+1}} \tag{5.14}$$

The virtual coupler of the haptic system is chosen to be a 2 parameter controller where k_c represents the stiffness and b_c is related to the damping. In order to keep the analysis simple, backward Euler transformation used in the controller.

$$Z_c(z) = k_c + b_c \left(\frac{Tz}{z-1} \right)^{\mu} \tag{5.15}$$

For the discrete time analysis, zero order hold is represented by $T/2(z+1)/z$ and the sampler is $1/T$. However, since hold and sampler are always used together throughout the analysis, the discrete time transfer function $ZOH(z)$ will be used.

$$ZOH(z) = \frac{1}{2} \frac{z+1}{z} \tag{5.16}$$

The hybrid mapping of the haptic interface, with the robot and the virtual coupler, is

$$\begin{bmatrix} F_h \\ -v_e^* \end{bmatrix} = \begin{bmatrix} Z_d(z) & ZOH(z) \\ -1 & 1/Z_c(z) \end{bmatrix} \begin{bmatrix} v_h \\ F_e^* \end{bmatrix} \tag{5.17}$$

If this 2-port network is absolutely stable and terminated by passive 1-port networks, then the resulting system will be passive. The absolute stability can be check by Llewellyn's criteria 1.

The first condition, $\Re p_{11} \geq 0$, is related to the robot and is satisfied for a physical system since $b > 0$. Second condition, on the other hand, is related to the virtual coupler model and we have the freedom choosing it. After some manipulations, the following inequality is obtained.

$$\frac{b_c + k_c T^{\mu} \frac{1}{2 \sin \frac{\omega T}{2}} \cos\left(\frac{\omega T - \pi}{2} \mu\right)}{b_c^2 + k_c^2 T^{2\mu} \frac{1}{4 \sin^2 \frac{\omega T}{2}} + k_c b_c \frac{1}{\sin \frac{\omega T}{2}} \cos\left(\frac{\omega T - \pi}{2} \mu\right)} \geq 0 \tag{5.18}$$

The third condition yields to

$$2b\frac{b_c + k_c T^{\mu}\frac{1}{2\sin\frac{\omega T}{2}}\cos\left(\frac{\omega T-\pi}{2}\mu\right)}{b_c^2 + k_c^2 T^{2\mu}\frac{1}{4\sin^2\frac{\omega T}{2}} + k_c b_c \frac{1}{\sin\frac{\omega T}{2}}\cos\left(\frac{\omega T-\pi}{2}\mu\right)} \geq 0.25 \tag{5.19}$$

After some manipulations of these inequalities the following corollary is found.

Corollary 2. *Consider a haptic system with a fractional order virtual coupler. The two-port network, consisting of the haptic display and the virtual coupler, is passive if*

$$8b_r \geq k_c + b_c\left(\frac{T}{2}\right)^{\mu} \tag{5.20}$$

5.3 Discussion

Calculus with integer order differointegrals has proved its ability to model the physical phenomena; but it is not the ultimate tool to model nature. In fact, fractional order calculus is an effective tool that broadens the modeling boundaries of the familiar calculus. Our proposition of using fractional calculus in haptics enables a new potential of rendering unorthodox impedances, such as viscoelastic materials that exhibit frequency dependent stiffness and damping characteristics within a single mechanical element. Even though approximate models for such materials with integer order differointegrals may exist, fractional order calculus is known to result in simpler and more capable models, capturing the true nature of such materials. Consequently, the use of fractional order calculus in haptics significantly extends the type of impedances that can be rendered using the integer order models.

Inclusion of fractional order models/controllers into the human-in-the-loop sampled data control loop has a direct consequence on the coupled stability characteristics of the overall system. In particular, Eq. 5.2 generalizes the well known passivity condition, $\delta > \frac{\kappa}{2} + \beta$ in the nondimensional form, to include factional order models. An important observation from this equation is the fact that the size of dimensionless κ-β passivity region can be modulated by tuning the order of the differointegral. Fig.5.1 provides a

visual demonstration of this result, where $\alpha = 1$ represents the virtual wall with integer order damping term. For $\alpha \in [0, 1)$, the fractional order differointegral term increases the nondimensional area of the κ-β passivity region. The minimum passivity region occurs as $\alpha \to 2$, where the fractional order element acts as a kinetic energy storage element (inertia).

5.4 Conclusions

We have proposed using fractional order models/controllers for haptic rendering and explored the impact of fractional order elements to the coupled stability of the overall sampled-data system. We also characterized the effective stiffness and damping behavior of the fractional order impedance as a function of frequency and differointegration order.

CHAPTER VI

TRANSPARENCY ANALYSIS

Rendering performance of a haptic system can be characterized by its transparency, where transparency refers to the match between the rendered virtual environment and impedance felt by the user.

Transparency can be analyzed by an effective impedance analysis to study the closed-loop impedance of the system with respect to the desired impedance for the rendered environment [24,25]. The effective impedances in terms of the parameters of the haptic system are defined as

$$\begin{aligned} ES(\omega) &= \omega \Im^{-}\{Z(j\omega)\} \\ &= m\omega^2 - K\cos\frac{\omega T}{2} - B\omega^{\mu}\cos\frac{\omega T - \pi\mu}{2} \end{aligned} \tag{6.1}$$

$$\begin{aligned} ED(\omega) &= \Re^{+}\{Z(j\omega)\} \\ &= b - \frac{K}{\omega}\sin\frac{\omega T}{2} - B\omega^{\mu-1}\sin\frac{\omega T - \pi\mu}{2} \end{aligned} \tag{6.2}$$

where force is considered as the input and velocity as the output.

Fig. 6.1 presents the interval of the angle $\omega T/2$ and how it changes with respect ot μ. Up to the Nyquist frequency, $\omega T/2$ is limited to the first quadrant; therefore, both $\cos\omega T/2$ and $\sin\omega T/2$ are positive for angles in this interval. However, the sign of sinus term changes for $0 \leq \mu \leq 1$ since the angle $(\omega T + \mu\pi)/2$ resides in the first and fourth quadrants. Finally, for $1 \leq \mu \leq 2$, the $\cos(\omega T + \mu\pi)/2$ term is always negative,

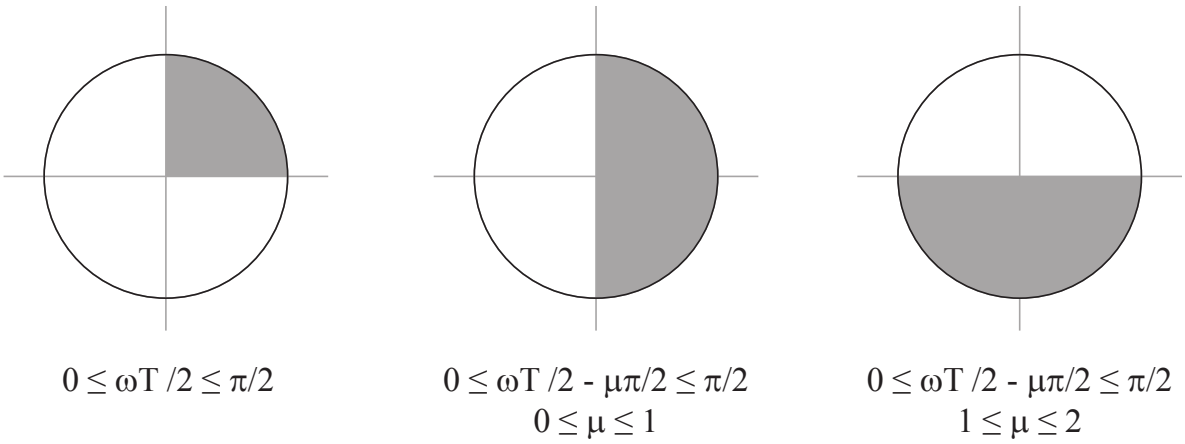

Figure 6.1: Change of the interval of ωT with respect to μ

whereas the sinus term can be positive or negative. This simple visualization is helpful for understanding the changes in the effective impedances presented in the following paragraphs.

Effective stiffness (ES) corresponds to the projection of the closed-loop impedance on the negative side of the imaginary axis. In the ES equation, the mass of the robot has a decreasing (deteriorating) effect on the stiffness rendering and these detrimental effects becomes more dominant as the frequency increases. The cosine term multiplying the virtual stiffness parameter is always positive but monotonically decreasing up to the Nyquist frequency $\omega_N = \pi/T$; hence virtual stiffness parameter contributes positively but in a decreasing fashion to the stiffness rendering in the frequency range $[0, \pi/T]$. The contribution of damping related term is slightly more involved due to the parameter μ. Up to Nyquist frequency, $0 \leq \omega \leq \pi/T$, the angle $\omega T/2$ resides in the first quadrant. By adding $-\pi\mu/T$ to this angle, $\omega T/2$ is rotated in the clockwise direction. If $0 \leq \mu \leq 1$ then this rotation is at most $90°$; hence in this frequency range, the sign of the cosine term multiplying B always stays positive. Therefore, one can conclude that when using a differentiation order $\mu \in [0, 1]$, the term B has a positive contribution to overall stiffness of rendering. On the other hand, if $1 < \mu \leq 2$, the rotation of the angle $\omega T/2$ in the clockwise direction is more than $90°$. In this case, the sign of $\cos \frac{\omega T - \pi\mu}{2}$ can be

negative for certain frequencies, resulting in a negative contribution to (deteriorating effect on) the effective stiffness of the closed-loop system.

Effective damping (ED) corresponds to the projection of the close-loop impedance on the positive side of the real axis. From this point of view, the physical damping b of the haptic interface always has a positive contribution to the effective damping. The stiffness of the virtual environment has a negative contribution to the effective damping, since the sign of $\sin \omega T/2$ is positive up to Nyquist frequency. However, this adverse effect is more significant for the low frequency range and phases out as the frequency increases. The contribution of the virtual damping related term can be analyzed in two parts. For $0 \leq \mu < 1$, the rotation of the angle $\omega T/2$, which resides in the first quadrant, is less than 90°; therefore, the sign of the term $\sin \frac{\omega T - \pi\mu}{2}$ can become both negative and positive. This implies that for certain frequency values, the virtual damping term will contribute to decrease the effective damping of the closed-loop system. Moreover, with this choice of μ, $\omega^{\mu-1}$ causes the contribution of the virtual damping be more significant for low frequency values. However, if $1 \leq \mu \leq 2$ the sign of $\sin \frac{\omega T - \pi\mu}{2}$ is always positive up to Nyquist frequency and the effect of the term B acts in favor of increasing the effective damping. Furthermore, with this choice of μ, this positive effect increases as the frequency increases due to the term $\omega^{\mu-1}$ which multiplies B.

As an example, consider a haptic device with $m = 0.65$ kg, $b = 3.5$ N s/m and virtual environment parameters $K = 50$ N/m and $B = 1$ N s/m. Fig. 6.2 depicts the effective stiffness and damping of the closed-loop impedance of this haptic system. An investigation of Fig. 6.2 may help materialize the observations presented.

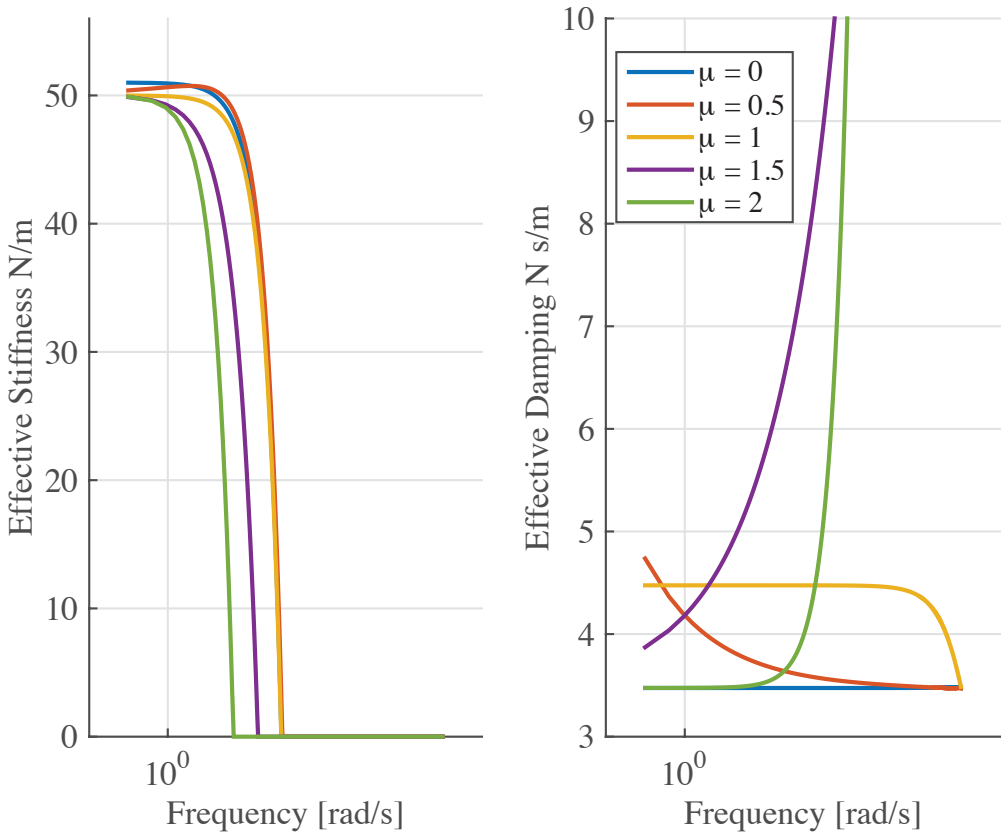

Figure 6.2: Effective impedance of a haptic system with $m = 0.65$ kg, $b = 3.5$ N s/mm, $K = 50$ N/m, $B = 1$ N s/m for various differentiation orders

6.1 Conclusion

Transparency analysis of the closed-loop haptic system reveals that using fractional order derivative may help rendering of stiffness values if the differentiation order if between 0 and 1, while contributing to the damping characteristic of the closed-loop system.

CHAPTER VII

HAPTIC RENDERING OF HUMAN PROSTATE

The theory introduced in the previous chapters can now be used for implementing fractional order dynamical systems for haptic rendering. As an example, haptic rendering of prostate tissue is presented in this section.

Mammal tissue exhibit viscoelastic behaviour that is one can observe creep and stress relaxation in these tissues. In the literature there are many viscoelastic models used for tissue modeling. Among them, fractional order models are considered in this dissertation.

In [2], a fractional order Kelvin-Voight model is used to model human prostate with and without cancer. The use of fractional order model introduces simplicity in number of parameters used in the model. On the other hand, fractional order models are good at capturing the stress relaxation property.

The mathematical model for healthy and cancerous prostate are

$$H_{\text{healthy}}(s) = 3.61s^{0.2154} \tag{7.1}$$

$$H_{\text{cancerous}}(s) = 8.65s^{0.2247} \tag{7.2}$$

In the haptic rendering experiments these models are implement and the fractional order derivatives are approximated by [54]. In order to capture the stress relaxation, two voice coil actuators, shown in Fig. 7.1, are used. On the blue VCA, the fractional order prostate model is implemented and the white VCA indents into the virtual prostate

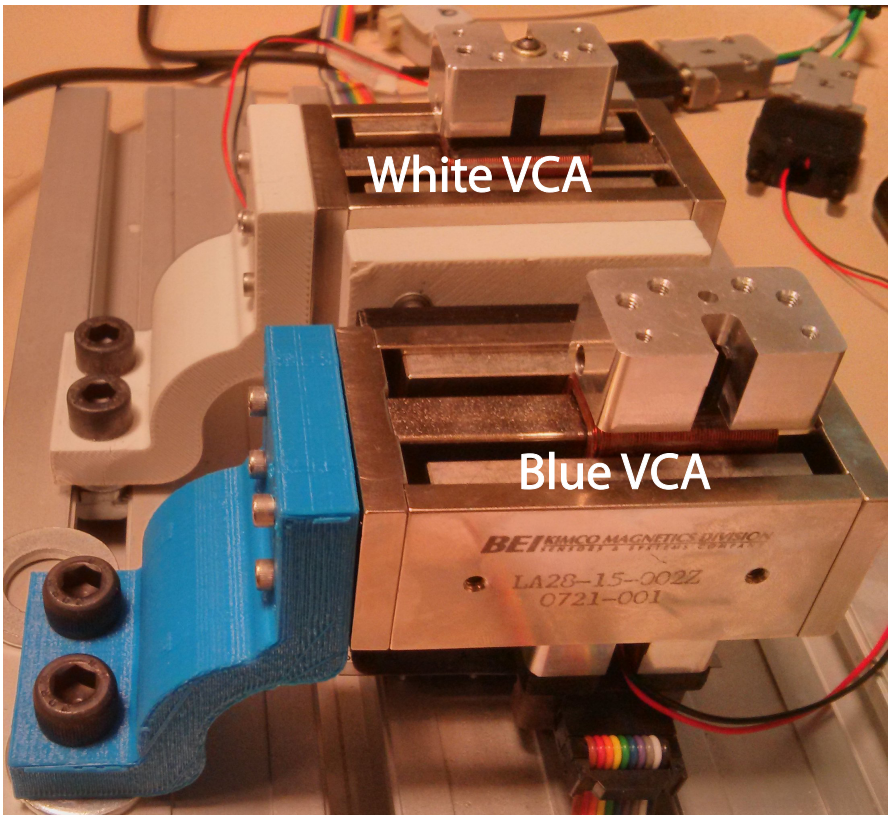

Figure 7.1: Voice coil actuators used in the stress relaxation experiments

model by physically pushing the blue VCA. For 200 s, the experiment is conducted and the current commanded to the blue VCA is recorded. This current information is used to estimate the force reaction of the virtual prostate model since the VCAs used in the experiments have low inertia and damping therefore, the current commanded is directly proportional to the force at the end effector. The stress relaxation of the virtual prostate with cancer is shown in Fig. 7.2. It can be seen from the figure that the haptic rendering of the prostate can clearly capture the true behaviour shown by the experimental results.

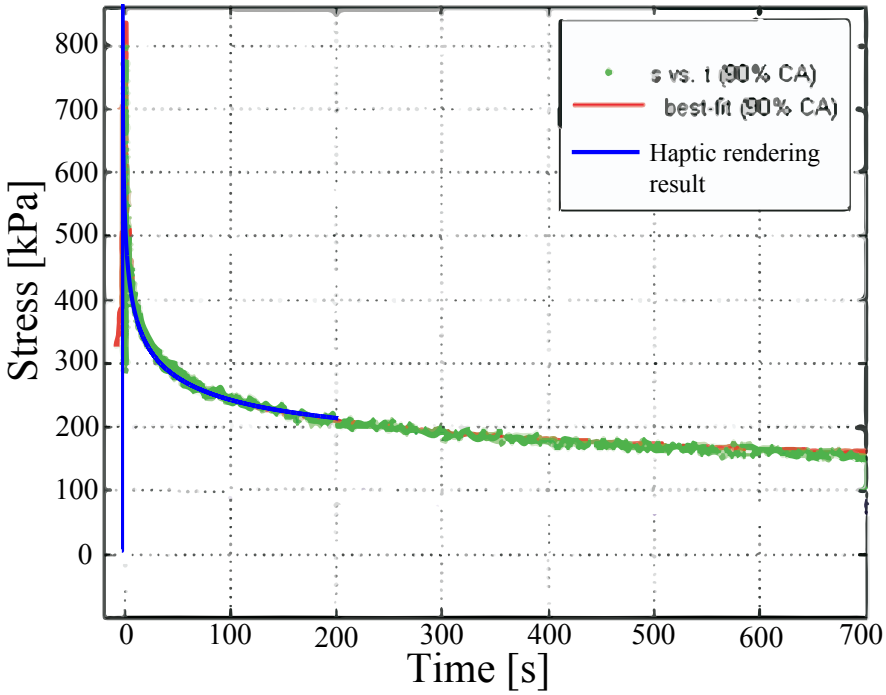

Figure 7.2: Stress relaxation of the cancerous prostate tissue

CHAPTER VIII

CONCLUSION AND FUTURE WORK

In this dissertation, we proposed the use fractional order controllers in haptic systems. A simple virtual environment model, consisting of a spring and a fractional order dissipative element, is used for understanding the efficacy of such controllers.

In the first analysis, we investigated the frequency dependent stiffness and damping characteristics of the fractional order environment model. Moreover, we introduced a proper nondimensionalization scheme for the haptic system parameters. Once an understanding of the new environment model is established, we conducted stability, passivity and transparency analysis on the haptic system.

We conducted stability analysis for a haptic system with and without a human operator. To conduct such analysis, the human is modeled using linear mass-spring-damper mechanical elements. Based on the stability analysis, we studied the effects of parameter changes on the stability regions.

A worst-case scenario for a haptic system occurs when the human operator is not present in the control loop. For this case, we analyzed the stability of the haptic system and experimentally verified the theoretical results. Our experiments were successful in capturing the stability region relations between different differentiation orders.

Due to the difficulty of modeling the human operator, we extend our analysis to a class of human operators, by studying the robust stability of the system using the passivity theory. We conducted passivity analysis on the haptic system with a passive human operator. First, we considered the passivity of the haptic display with the

virtual environment model and checked the passivity for this sampled-data system. Our passivity results provided a generalization of the existing passivity conditions. We also extended the passivity analysis of the haptic system to complex, but passive, environments. We showed that the haptic system with fractional order virtual coupler can be made passive for certain differentiation orders.

We concluded the theoretical analysis by investigating the transparency performance of the haptic system in terms of effective impedance. We showed that for a passive haptic system, the differentiation order used in the virtual coupler should be less than or equal to 1. On the other hand, higher differentiation orders lead to better dissipation characteristics.

Finally, we have applied the theoretical knowledge on a real world example and presented the haptic rendering of human prostate which exhibits viscoelastic properties and can be modeled with fractional order calculus. We showed the success of the rendering by comparing the stress relaxation of the real prostate to the virtual one.

As a natural extension of the two port analysis, future work includes analysis of teleoperation architectures and the effect of fractional order elements in time delayed teleoperation.

BIBLIOGRAPHY

[1] A. Carpinteri and F. Mainardi, *Fractals and Fractional Calculus in Continuum Mechanics*. Springer Verlag, 1997.

[2] M. Zhang, P. Nigwekar, B. Castaneda, K. Hoyt, J. V. Joseph, A. di Sant'Agnese, E. M. Messing, J. G. Strang, D. J. Rubens, and K. J. Parker, "Quantitative characterization of viscoelastic properties of human prostate correlated with histology," *Ultrasound in Medicine & Biology*, vol. 34, no. 7, pp. 1033 – 1042, 2008.

[3] S. T. Taylor, A. L. Lerner, D. J. Rubens, and K. J. Parker, "A kelvin-voight fractional derivative model for viscoelastic characterization of liver tissue," in *ASME International Mechanical Engineering Congress and Exposition*, 2002, pp. 447–448.

[4] Y. Kobayashi, P. Moreira, C. Liu, P. Poignet, N. Zemiti, and M. Fujie, "Haptic feedback control in medical robots through fractional viscoelastic tissue model," in *Annual International Conference of the IEEE Engineering in Medicine and Biology Society*, 2011, pp. 6704–6708.

[5] M. Minsky, O.-y. Ming, O. Steele, F. P. Brooks, Jr., and M. Behensky, "Feeling and seeing: Issues in force display," in *Proceedings of the Symposium on Interactive 3D Graphics*, 1990, pp. 235–241.

[6] R. B. Gillespie and M. R. Cutkosky, "Stable user-specific haptic rendering of the virtual wall," in *Proc. Int. Mechanical Engineering Congress and Exhobotion*, 1995.

[7] J. Gil, A. Avello, A. Rubio, and J. Florez, "Stability analysis of a 1 dof haptic interface using the routh-hurwitz criterion," *IEEE Transactions on Control Systems Technology*, vol. 12, no. 4, pp. 583–588, 2004.

[8] T. Hulin, C. Preusche, and G. Hirzinger, "Stability boundary for haptic rendering: Influence of physical damping," in *IEEE/RSJ International Conference on Intelligent Robots and Systems*, 2006, pp. 1570–1575.

[9] ——, "Stability boundary for haptic rendering: Influence of human operator," in *IEEE/RSJ International Conference on Intelligent Robots and Systems*, 2008, pp. 3483–3488.

[10] T. Hulin, A. Albu-Schaffer, and G. Hirzinger, "Passivity and stability boundaries for haptic systems with time delay," *IEEE Transactions on Control Systems Technology*, vol. PP, no. 99, pp. 1–1, 2013.

[11] N. Diolaiti, G. Niemeyer, F. Barbagli, and J. Salisbury, "Stability of haptic rendering: Discretization, quantization, time delay, and coulomb effects," *IEEE Transactions on Robotics*, vol. 22, no. 2, pp. 256–268, 2006.

[12] N. Hogan, "Controlling impedance at the man/machine interface," in *IEEE International Conference on Robotics and Automation*, 1989, pp. 1626–1631.

[13] R. Anderson and M. Spong, "Bilateral control of teleoperators with time delay," *IEEE Transactions on Automatic Control*, vol. 34, no. 5, pp. 494–501, 1989.

[14] J. E. Colgate and G. G. Schenkel, "Passivity of a class of sampled-data systems: Application to haptic interfaces," *Journal of Robotic Systems*, vol. 14, no. 1, pp. 37–47, 1997.

[15] J. Colgate, M. Stanley, and J. Brown, "Issues in the haptic display of tool use," in *IEEE/RSJ International Conference on Intelligent Robots and Systems. 'Human Robot Interaction and Cooperative Robots'*, vol. 3, 1995, pp. 140–145.

[16] R. J. Adams and B. Hannaford, "Stable haptic interaction with virtual environments," *IEEE Transactions on Robotics and Automation*, vol. 15, no. 3, pp. 465–474, 1999.

[17] J.-P. Kim and J. Ryu, "Robustly stable haptic interaction control using an energy-bounding algorithm," *The International Journal of Robotics Research*, 2009.

[18] G. Leung, B. Francis, and J. Apkarian, "Bilateral controller for teleoperators with time delay via μ-synthesis," *IEEE Transactions on Robotics and Automation*, vol. 11, no. 1, pp. 105–116, 1995.

[19] J. Yan and S. Salcudean, "Teleoperation controller design using h infin;-optimization with application to motion-scaling," *IEEE Transactions on Control Systems Technology*, vol. 4, no. 3, pp. 244–258, 1996.

[20] D. Lawrence, "Stability and transparency in bilateral teleoperation," *IEEE Transactions on Robotics and Automation*, vol. 9, no. 5, pp. 624–637, 1993.

[21] S. Hirche, A. Bauer, and M. Buss, "Transparency of haptic telepresence systems with constant time delay," in *IEEE Conference on Control Applications*, 2005, pp. 328–333.

[22] P. Griffiths, R. Gillespie, and J. Freudenberg, "A fundamental tradeoff between performance and sensitivity within haptic rendering," *IEEE Transactions on Robotics*, vol. 24, no. 3, pp. 537–548, 2008.

[23] ——, "A fundamental linear systems conflict between performance and passivity in haptic rendering," *IEEE Transactions on Robotics*, vol. 27, no. 1, pp. 75–88, 2011.

[24] J. Mehling, J. Colgate, and M. Peshkin, "Increasing the impedance range of a haptic display by adding electrical damping," in *First Joint Eurohaptics Conference and Symposium on Haptic Interfaces for Virtual Environment and Teleoperator Systems. World Haptics*, 2005, pp. 257–262.

[25] N. Colonnese, S. Sketch, and A. Okamura, "Closed-loop stiffness and damping accuracy of impedance-type haptic displays," in *IEEE Haptics Symposium (HAPTICS)*, 2014, pp. 97–102.

[26] L. Stocco, S. E. Salcudean, and F. Sassani, "Fast constraint global minimax optimization of robot parameters," *Robotica*, vol. 16, pp. 595–606, 1998.

[27] R. Unal, G. Kiziltas, and V. Patoglu, "A multi-criteria design optimization framework for haptic interfaces," in *Symposium on haptic interfaces for virtual environment and teleoperator systems*, 2008, pp. 231–238.

[28] R. Kurtz and V. Hayward, "Multiple-goal kinematic optimization of a parallel spherical mechanism with actuator redundancy," *IEEE Transactions on Robotics and Automation*, vol. 8, no. 5, pp. 644–651, 1992.

[29] B. Hannaford and J.-H. Ryu, "Time-domain passivity control of haptic interfaces," *IEEE Transactions on Robotics and Automation*, vol. 18, no. 1, pp. 1–10, 2002.

[30] J.-H. Ryu, D.-S. Kwon, and B. Hannaford, "Stable teleoperation with time-domain passivity control," *IEEE Transactions on Robotics and Automation*, vol. 20, no. 2, pp. 365–373, 2004.

[31] K. B. Fite, M. Goldfarb, and A. Rubio, "Loop shaping for transparency and stability robustness in time-delayed bilateral telemanipulation," *J. Dyn. Sys., Meas., Control*, vol. 126, no. 3, pp. 650–656, 2003.

[32] S. Buerger and N. Hogan, "Complementary stability and loop shaping for improved human -robot interaction," *IEEE Transactions on Robotics*, vol. 23, no. 2, pp. 232–244, 2007.

[33] A. Haddadi and K. Hashtrudi-Zaad, "Bounded-impedance absolute stability of bilateral teleoperation control systems," *IEEE Transactions on Haptics*, vol. 3, no. 1, pp. 15–27, 2010.

[34] R. L. Bagley and P. J. Torvik, "Fractional calculus – a different approach to the anaylsis of viscoelastically damped structures," *AIAA J.*, vol. 21, pp. 741 – 748, 1983.

[35] A. Oustaloup, B. Mathieu, and P. Lanusse, "The crone control of resonant plants: Application to a flexible transmission," *European Journal of Control*, vol. 1, no. 2, pp. 113 – 121, 1995.

[36] I. Podlubny, "Fractional-order systems and pi/sup /spl lambda//d/sup /spl mu//-controllers," *IEEE Transactions on Automatic Control*, vol. 44, no. 1, pp. 208–214, 1999.

[37] B. J. Lurie, "Three-parameter tunable tilt-integral-derivative (tid) controller," USA Patent US 5 371 670 A, 1994.

[38] D. Xue and Y.-Q. Chen, "A comparative introduction of four fractional order controllers," in *4th World Congress on Intelligent Control and Automation*, vol. 4, 2002, pp. 3228–3235.

[39] C. Ma and Y. Hori, "Fractional-order control: Theory and applications in motion control [past and present]," *IEEE Industrial Electronics Magazine*, vol. 1, no. 4, pp. 6–16, 2007.

[40] N. M. F. Ferreira and J. A. T. Machado, "Fractional-order hybrid control of robotic manipulators," in *International Conference on Advanced Robotics*, 2003.

[41] Y. Luo and Y. Q. Chen, *Fractional order motion controls*. Wiley, 2012.

[42] I. Petras, *Fractional-order nonlinear systems*. Springer, 2011.

[43] C. A. Monje, Y. Q. Chen, B. M. Vinagre, D. Xue, and V. Feliu-Batlle, *Fractional-order systems and controls: fundamentals and applications*. Springer, 2010.

[44] R. Caponetta, G. Dongola, L. Fortuna, and I. Petras, *Fractional order systems*. World Scientific, 2010.

[45] K. B. Oldham and J. Spanier, *The Fractional Calculus*. Academic Press, 1974.

[46] Y.-Q. Chen, I. Petras, and D. Xue, "Fractional order control - a tutorial," in *American Control Conference*, 2009, pp. 1397–1411.

[47] C. Li and F. Zhang, "A survey on the stability of fractional differential equations," *The European Physical Journal Special Topics*, vol. 193, no. 1, pp. 27–47, 2011.

[48] B. Krishna, "Studies on fractional order differentiators and integrators: A survey," *Signal Processing*, vol. 91, no. 3, pp. 386 – 426, 2011.

[49] M. Efe, "Fractional order systems in industrial automation 2014;a survey," *IEEE Transactions on Industrial Informatics*, vol. 7, no. 4, pp. 582–591, 2011.

[50] J. T. Machado, V. Kiryakova, and F. Mainardi, "Recent history of fractional calculus," *Communications in Nonlinear Science and Numerical Simulation*, vol. 16, no. 3, pp. 1140 – 1153, 2011.

[51] T. Hulin, A. Albu-Schaffer, and G. Hirzinger, "Passivity and stability boundaries for haptic systems with time delay," *IEEE Transactions on Control Systems Technology*, vol. 22, no. 4, pp. 1297–1309, July 2014.

[52] I. Podlubny, I. Petras, B. M. Vinagre, P. O'Leary, and L. Dorcak, "Analogue realizations of fractional-order controllers," *Nonlinear Dynamics*, vol. 29, 2002.

[53] Y.-Q. Chen and K. Moore, "Discretization schemes for fractional-order differentiators and integrators," *IEEE Transactions on Circuits and Systems I: Fundamental Theory and Applications*, vol. 49, no. 3, pp. 363–367, 2002.

[54] A. Oustaloup, F. Levron, B. Mathieu, and F. Nanot, "Frequency-band complex noninteger differentiator: characterization and synthesis," *IEEE Transactions on Circuits and Systems I: Fundamental Theory and Applications*, vol. 47, no. 1, pp. 25–39, 2000.

[55] M. Al-Alaoui, "Novel iir differentiator from the simpson integration rule," *IEEE Transactions on Circuits and Systems I: Fundamental Theory and Applications*, vol. 41, no. 2, pp. 186–187, 1994.

[56] R. S. Barbosa, J. T. Machado, and M. F. Silva, "Time domain design of fractional differintegrators using least-squares," *Signal Processing*, vol. 86, no. 10, pp. 2567 – 2581, 2006.

[57] S. Das and I. Pan, *Fractinal Order Signal Processing: Introductory Concepts and Applications*. Springer, 2012.

[58] M. D. Ortigueira, *Fractional Calculus for Scientists and Engineers*. Springer, 2011.

[59] J. Colgate, P. Grafing, M. Stanley, and G. Schenkel, "Implementation of stiff virtual walls in force-reflecting interfaces," in *Virtual Reality Annual International Symposium*, 1993, pp. 202–208.

[60] J. Colgate and J. Brown, "Factors affecting the z-width of a haptic display," in *IEEE International Conference on Robotics and Automation*, vol. 4, 1994, pp. 3205–3210.

[61] D. Weir, J. Colgate, and M. Peshkin, "Measuring and increasing z-width with active electrical damping," in *Symposium on Haptic interfaces for virtual environment and teleoperator systems*, 2008, pp. 169–175.

[62] D. Liu, O. Gibaru, W. Perruquetti, and T. Laleg-Kirati, "Fractional order differentiation by integration and error analysis in noisy environment," *Automatic Control, IEEE Transactions on*, vol. PP, no. 99, pp. 1–1, 2015.